PLAN B INDEPENDENT STUDY

DEVELOPMENT OF A PREDICTIVE SIMULATION WORKFLOW FOR A 1L HYDROGEN-

FUELED ENGINE

Submitted by

Antoine Bertrand

Department of Mechanical Engineering

In partial fulfillment of the requirements

For the Degree of Master of Science

Colorado State University

Fort Collins, Colorado

Summer 2025

Master's Committee:
      Advisor: Bret Windom

      Daniel Olsen
      Thomas Bradley

ABSTRACT

DEVELOPMENT OF A PREDICTIVE SIMULATION WORKFLOW FOR A 1L HYDROGEN-FUELED ENGINE

This project focuses on the development of a hydrogen-fueled internal combustion engine (ICE) as part of the ARPA-e INTEGRATE initiative, which aims to couple Solid Oxide Fuel Cells (SOFCs) with ICEs to create a more robust and cost-effective hybrid power system. The specific objective is to convert a diesel-derived engine to operate on pure hydrogen, with a target output of over 10 kW and a brake thermal efficiency of 35%.

The first phase of the work addresses piston redesign to accommodate hydrogen combustion. This includes modifying the compression ratio and conducting thermal and structural finite element analyses (FEA) to ensure the redesigned piston can withstand the unique thermal loads and mechanical stresses associated with hydrogen operation.

The second phase presents a predictive simulation protocol combining 3D computational fluid dynamics (CFD) using CONVERGE CFD with 1D engine system modeling in GT-Power. This approach enables an evaluation of optimal engine operating conditions and assesses whether the simulated performance meets the targets defined by the ARPA-e INTEGRATE project.

ACKNOWLEDGEMENTS

TABLE OF CONTENTS

LIST OF TABLES

LIST OF ACRONYMS

ICE .... Internal Combustion Engine

SOFC .... Solid Oxide Fuel Cell

DI .... Direct Injection

PFI .... Port Fuel Injection

SI .... Spark-Ignited

CFD ....Computational Fluid Design

CR .... Combustion Ratio

FEA ....Finite Element Analysis

OEM ....Original Equipment Manufacturer

SOC ....Start of Combustion

MFB ....Mass Fraction Burned

CA50 .... Crank Angle at 50% fuel burned

CAD .... Computer Aided Design

OHV .... Overhead Camshaft

KI .... Knock Intensity

TDC .... Top Dead Center

BDC .... Bottom Dead Center

AlSi12 .... Aluminum Silicon 12% alloy

OLS ....Ordinary Least Squares

SSR .... Sum of Squared Residuals

UTS .... Ultimate Tensile Strength

SF .... Safety Factor

TPA .... Three-Pressure Analysis

SMF .... Species Mass Fraction

MFB ....Mass Fraction Burned

RPM .... Revolutions Per Minute

AFR ....Air-to-Fuel Ratio

AMR .... Adaptive Mesh Refinement

SGS .... Sub-Grid Scale

C3 .... Computational Chemistry Consortium

ECFM-3Z .... Extended Coherent Flame Model, three Zones

DNS .... Direct Numerical Simulation

RANS .... Reynolds-Averaged Navier–Stokes

IVO .... Intake Valve Opening

IVC .... Intake Valve Closing

EVO .... Exhaust Valve Opening

EVC .... Exhaust Valve Closing

CA .... Crank Angle

N_2 .... Nitrogen

O_2 ....Oxygen

H_2 .... Hydrogen

HRR .... Heat Release Rate

NA .... Naturally Aspirated

1. INTRODUCTION

1.1 Motivations

1.1.1 Context

Developing a detailed methodology to predict the performance of a diesel-to-hydrogen internal combustion engine (ICE) conversion is justified from both ecological and economic perspectives. Although hydrogen fuel cells typically offer higher efficiency in converting hydrogen into electrical energy (see *Figure 1*), hydrogen-fueled ICEs present a more practical and sustainable alternative for certain applications. This is particularly true when considering the opportunity to repurpose existing diesel engine platforms, thereby reducing both manufacturing costs and environmental impact. Instead of designing hydrogen ICEs from the ground up, adapting existing engines extends their useful life and leverages already-available infrastructure. For these reasons, hydrogen engine retrofits often represent a more feasible and scalable solution in the transition toward carbon-neutral mobility.

Figure 1: Average powertrain efficiency for HICEV vs. HFCV for the WLTP (Worldwide harmonized Light vehicles Test Procedure) drive cycle, the region of low and medium speeds (WLTP-LS), and the region of high and extra-high speeds (WLTP-HS) [1]

1.1.2 Integration Within the ARPA-e INTEGRATE Project Framework

Although the motivation to retrofit a diesel engine for hydrogen combustion is compelling on its own, this engine development is also part of a broader initiative known as the ARPA-e INTEGRATE Project. This project addresses the limitations of solid oxide fuel cell (SOFC) in commercial distributed power generation, which include high capital costs, poor durability, and moderate system efficiency, primarily due to their historically high operating temperatures (750–1000 °C). While advancements have been made, challenges such as expensive balance-of-plant components and limited efficiency (typically 40–45%) still hinder widespread adoption. To overcome these barriers, the ARPA-e INTEGRATE Project proposes a novel hybrid system that couples low-temperature, metal-supported SOFC with a hydrogen-fueled ICE. This fully integrated solution aims to offer a cost-effective, robust, and dynamically responsive power system tailored for distributed energy applications (see *below*).
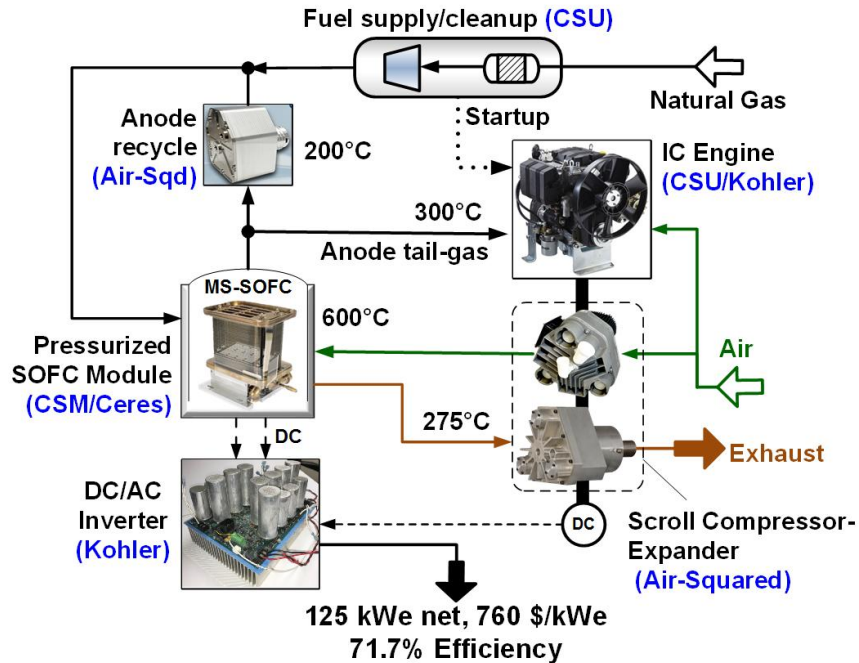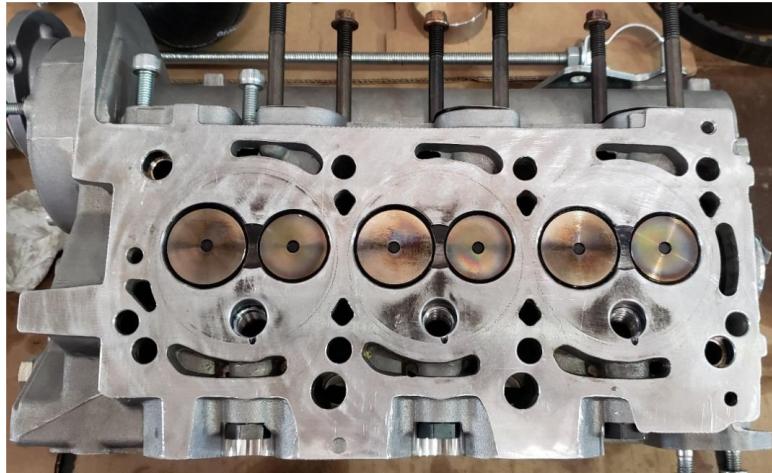
Figure 2: Proposed SOFC/ICE Hybrid System & Supply Scope [2]

In the ARPA-e INTEGRATE system, the SOFC unit is coupled with an ICE, which replaces the conventional catalytic combustor and is fueled by the anode tail-gas to generate additional power. The system leverages pressurized SOFC air supply and gas expansion through innovative rotating equipment that combines balance-of-plant functions, simplifies control strategies, and removes the need for expensive high-speed electric generators. Furthermore, the use of low-temperature, metal-supported SOFC with high internal reforming capability (>85%) significantly reduces the thermal load on heat exchangers, lowering material requirements and overall recuperator costs. In this pressurized configuration (~3 bar) with 82% fuel utilization and a 35% efficient engine, the hybrid system can reach a net thermal efficiency of nearly 72% (LHV) at a projected capital cost of just $760/kW.

As part of this effort, a preliminary focus is placed on the development of a hydrogen-fueled ICE. The goal is to assess whether a converted diesel engine can operate on pure hydrogen, under naturally aspirated conditions and standard intake temperature, while reaching a power output of 10 kW with an efficiency target of 30%. Although the long-term configuration will include boosting and temperature control (e.g., chillers or intercoolers), this initial phase aims to validate the engine's baseline capabilities and performance on hydrogen alone.

1.1.3   Previous Work on Engine Development

The ARPA-e INTEGRATE Project began in 2019, and as of 2025, engine development has already achieved several key milestones. The engine, originally a direct injection diesel (DI), has been successfully converted into a port fuel injected (PFI), spark-ignited (SI), hydrogen-fueled engine (see Section 2.1.1 for details on the conversion process). The cylinder head was also modified to accommodate a spark plug in place of the original diesel injector (see *Figure 3*).

Figure 3: Modified cylinder head of the original direct injection (DI) diesel engine to accommodate a spark plug in place of the injector [3].

In parallel, a predictive simulation model of the same engine architecture was previously developed by Matthew Countie [3]. However, it is important to note that while the model used the same engine block, it operated on boosted natural gas rather than pure hydrogen. Although some progress has been made toward the development of a hydrogen internal combustion engine, no experimental testing has yet been performed using pure hydrogen, only tail gas or hydrogen-blended fuel mixtures have been used so far.

1.1.4   Justification for Fully Predictive Modeling
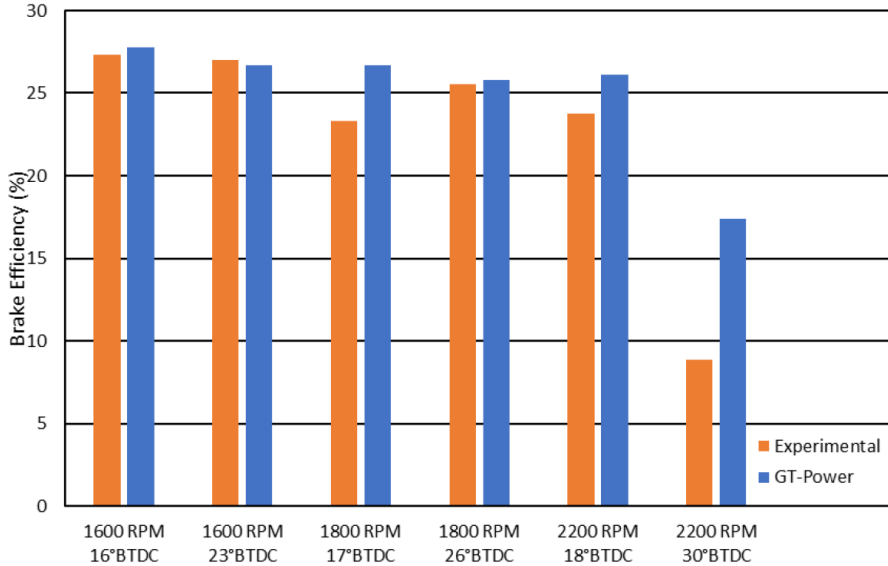
Due to the absence of experimental data for hydrogen combustion in this engine, the conventional approach for creating a 0D/1D model, as typically proposed by GT-Power, is not directly applicable. In particular, the lack of combustion-specific measurements prevents the calibration of commonly used predictive models such as SI Turb.

To overcome this limitation, an alternative strategy is adopted: the combustion process is first simulated using 3D Computational Fluid Dynamics (CFD), and the resulting data is then translated into a 1D combustion object compatible with GT-Power. This methodology relies solely on engine geometry and physical modeling, requiring no empirical calibration, which makes it a fully predictive and robust approach, particularly well-suited for early-phase hydrogen engine development where test data is unavailable.

1.2 Literature review

1.2.1   Previous Thesis on the Engine

The thesis by Matthew Countie, titled <u>Predictive Modeling and Testing of a Diesel-Derived Solid Oxide Fuel Cell Tail Gas Spark-Ignition Engine</u> [3], was conducted on the Kohler KDW993T, the turbocharged version of the KDW1003 engine used in this study. Both engines share identical core architecture, allowing for direct transference of modeling and geometrical data. This prior work significantly contributed to the understanding of the engine's behavior and was especially helpful in the development of the GT-Power model used in the present study. 1D conversions of key components such as the intake and exhaust runners as well as the cooling circuit geometry had already been completed.

Figure 4: Countie's GT-Power model results, showing correlation between Experimental and Simulated Brake Efficiency [3].

Countie's results demonstrated a strong correlation between GT-Power simulations and experimental data, validating the accuracy of his approach (see *Figure 4*). While his model was calibrated for tail gas combustion, it serves as a reliable foundation for building the pure hydrogen-based GT-Power model developed in this work.

1.2.2   Convergent Science: Converge CFD for H2 Modelling

The software selected for combustion modeling, which is the most critical component of the predictive approach, is Converge CFD. This choice was guided in part by insights gained from the webinar Converge for H$_2$ Modelling: IC Engines [4], which provided valuable guidance on best practices for simulating hydrogen combustion. The webinar addressed key aspects of model setup, including the selection of combustion and turbulence models as well as strategies for grid mesh control (more details in Section 3.2.2).

1.3 Objectives and overview

1.3.1   Objectives

This thesis builds upon a diesel engine that has already undergone preliminary modifications for hydrogen combustion. The only remaining design change concerns the piston, which is addressed in detail in Section 4. As such, the first set of objectives focuses on the mechanical redesign of the engine:

- Redesign the piston head to achieve a compression ratio (CR) of 10:1

- Verify whether the new design can withstand thermal and mechanical stress during combustion using Finite Element Analysis (FEA)

The second focus of the thesis is the development of a fully predictive combustion model. The goals associated with this modeling approach are:

- Create a combustion map to identify regions of optimal engine efficiency

- Evaluate the engine's performance output, particularly its ability to reach 10 kW of power with 30% efficiency under naturally aspirated conditions

- Establish a generalized methodology for predictive combustion modeling that can be adapted to different fuel blends and engine platforms

1.3.2 Overview of the Piston Design
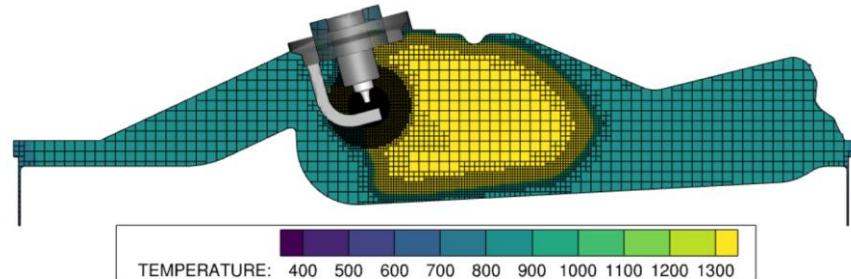
The conversion of a diesel engine to operate on hydrogen fuel requires substantial modifications to the piston geometry due to the fundamental differences in combustion characteristics between the two fuels. Diesel engines rely on high compression ratios and direct injection combustion, while hydrogen combustion is premixed and highly reactive, necessitating a lower compression ratio and a more uniform pressure distribution. This section of the thesis focuses on the redesign of the OEM piston to meet the new operational requirements, ensuring both structural integrity and thermal performance under hydrogen combustion. The redesigned piston is evaluated through detailed geometric modeling, thermodynamic volume calculations, and coupled thermal–mechanical finite element analyses. These steps are essential to validate the feasibility of the modified design before any physical prototyping or testing is conducted.

OEM Design   Modified Design

Figure 5: Comparison between the Original (OEM) piston head design with a CR of 28:1 and the modified design with a CR of 10:1.

1.3.3 Overview of Predictive Modeling

Due to the limited availability of experimental data for hydrogen internal combustion engines, this work proposes a fully predictive simulation methodology for hydrogen-fueled combustion using a combination of 3D CFD and 1D engine modeling. The objective is to create a combustion model based solely on engine geometry and fundamental physics, without the need for experimental calibration. A series of CFD simulations is performed using CONVERGE CFD to model the combustion process for various equivalence ratios (Φ) and spark timings (SOC). The resulting Mass Fraction Burned (MFB) curves are interpolated into a continuous map and integrated into GT-Power to predict engine performance. This methodology allows the identification of optimal operating conditions, such as a constant CA50, and provides a validated tool for evaluating engine behavior under different hydrogen fueling strategies.

Figure 6: Example of a 3D CFD simulation of the H2 combustion made using CONVERGE CFD

Software [4].

2. PISTON DESIGN

2.1 New CAD Design

To accommodate the conversion to hydrogen fuel, the engine originally designed for diesel combustion requires several modifications. While some of these changes have already been implemented, the piston head still needs to be redesigned to suit the specific requirements of hydrogen combustion.

2.1.1   Kohler 1L KDW1003

Figure 7: Isometric view of the unmodified KDW1003.

The engine used in this project is a Kohler KDW1003, a 1-liter, three-cylinder inline diesel engine. It is a four-stroke engine with a cast iron block and an aluminum cylinder head, featuring an overhead camshaft (OHC) configuration. The engine specifications are summarized in the *Table 1*.
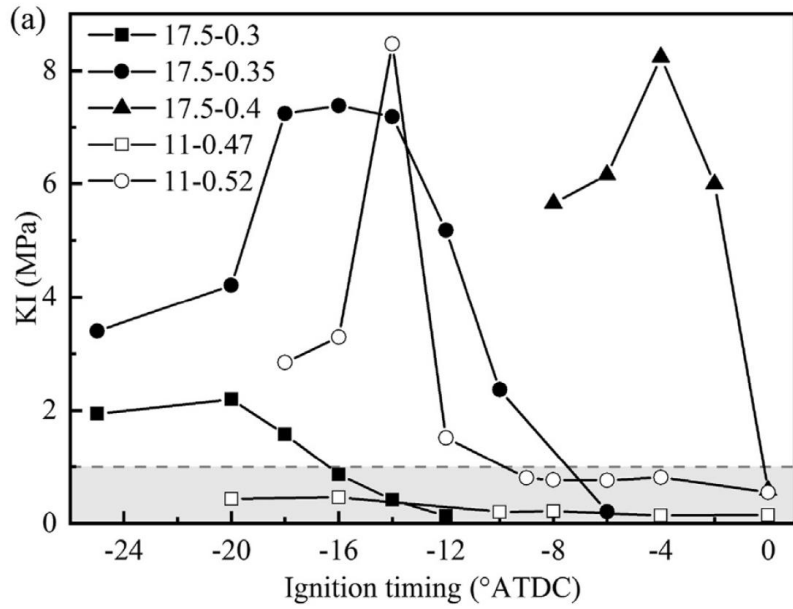
Table 1: Original Kohler diesel engine specs

MODEL		KDW1003
GROSS POWER @ RPM	max. hp (kw)	23.7 (17.7) @ 3600
DISPLACEMENT	cu in (cc)	62.7 (1028)
BORE	in (mm)	3 (75)
STROKE	in (mm)	3.1 (77.6)
CYLINDERS		3
PEAK TORQUE @ RPM	ft-lb (Nm)	36.8 (50) @ 2600
COMPRESSION RATIO		22.8:1
DRY WEIGHT	lb (kg)	187.6 (85)
OIL CAPACITY	U.S. qt (L)	2.5 (2.4)
DIMENSIONS	in (mm)	20.2 x 16.2 x 20.3 (513 x 412 x 516)

The KDW1003 engine, as originally designed, features a DI system optimized for diesel combustion. For the purposes of this project, the engine was converted to operate using hydrogen with PFI. This required modifying the cylinder head to accommodate spark plugs, replacing the original diesel injectors. The conversion from compression ignition to SI is a critical step in enabling hydrogen combustion, as hydrogen's high reactivity makes it unsuitable for uncontrolled autoignition typical of diesel engines. These modifications also support applications involving tail-gas utilization in hybrid SOFC-ICE systems.

2.1.2 Motivation to Change the Compression Ratio

By design, diesel engines operate with a high compression ratio, typically around 21:1, to promote the autoignition of the fuel. However, hydrogen is significantly more reactive than diesel and is highly prone to knock or pre-ignition under such high-pressure conditions. To avoid uncontrolled combustion, the ignition timing must be actively managed using a spark plug, and the compression ratio must be reduced to ensure stable and controlled operation.

Figure 8: Variations in Knock Intensity (KI) with ignition timing under different equivalence ratios and CR [5].

Studies have shown that, in the case of hydrogen combustion, a lower CR is generally more beneficial [5]. While higher CRs typically lead to improved thermal efficiency in conventional engines, hydrogen's high reactivity introduces a significant risk of engine knock. This knock reduces the proportion of energy converted into useful work, as more energy is lost through pressure oscillations. The referenced study demonstrated that reducing the CR from 17.5:1 to 11:1 led to a significant decrease in the knock intensity (KI) (see *Figure 8*). Based on prior development work on this engine, the lowest practical CR achievable is 10:1. This marks a substantial reduction from the engine's original compression ratio of 22.8:1, making it more suitable for hydrogen operation.

2.1.3 Design of the Piston Head

Piston head designed for efficient diesel combustion
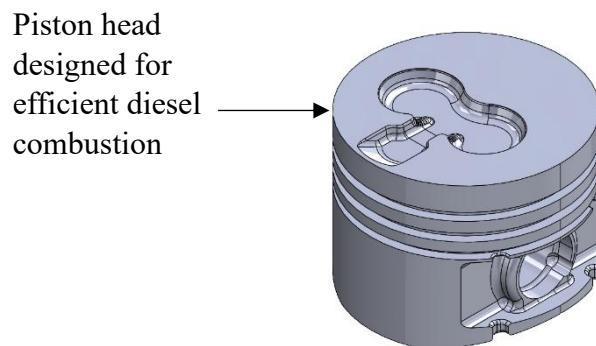
Figure 9: OEM Piston head design.

In addition, the piston head geometry in a conventional diesel engine is specifically designed to promote air-fuel mixing during direct injection (see *Figure 9*), where liquid diesel fuel is injected late into the cycle and does not require premixing. However, this design is incompatible with hydrogen combustion, which relies on a premixed, homogeneous fuel-air mixture to achieve uniform flame propagation and reduce the risk of abnormal combustion phenomena. As a result, the piston head must be redesigned to support more homogeneous combustion and to ensure a more uniform distribution of pressure forces during the expansion stroke.
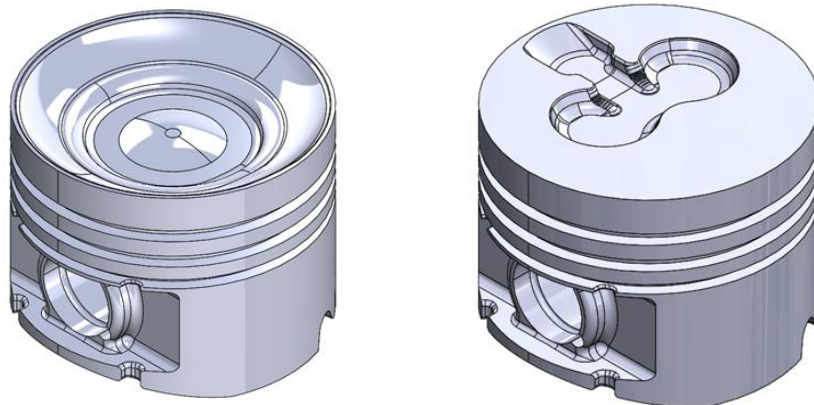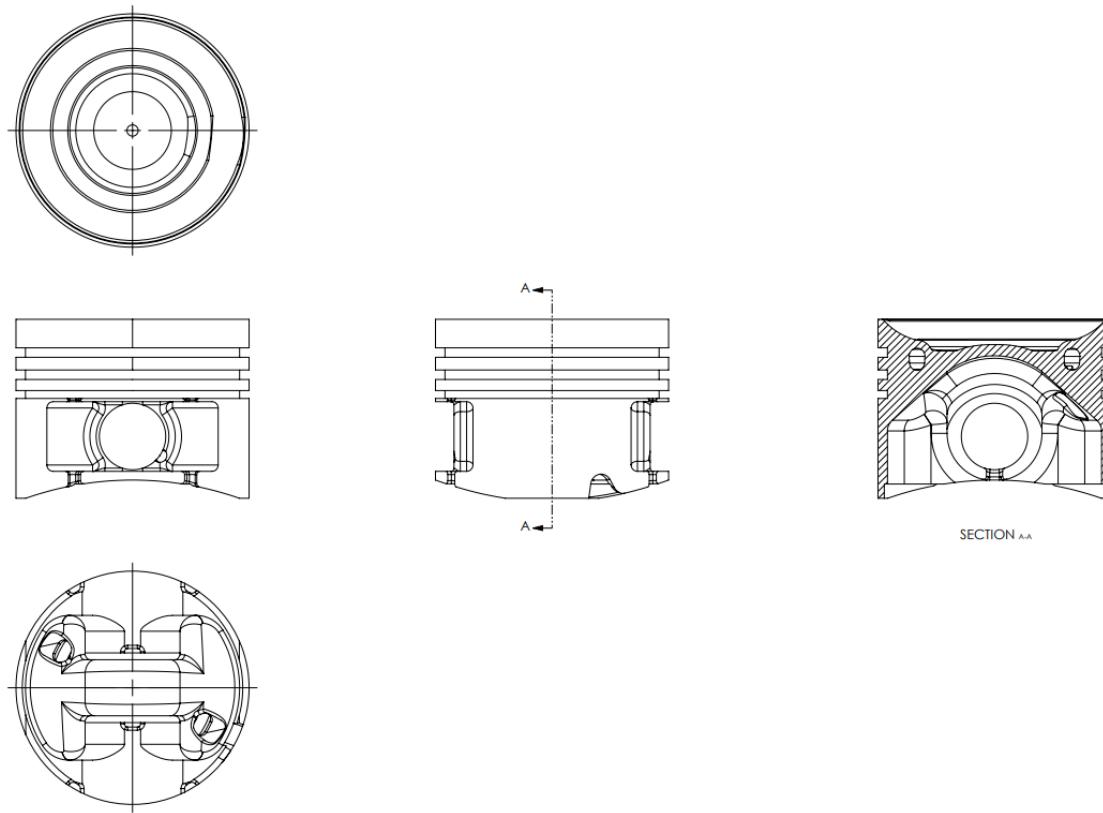
Figure 10: Volume comparison between OEM design (Right) and the modified design (Left).

The redesigned piston features central symmetry, allowing combustion forces to be evenly distributed across the piston crown and thereby reducing the likelihood of localized stress concentrations or mechanical failure. To reach the target compression ratio of 10:1, the approximate volume difference between the OEM diesel piston and the modified design was estimated. This provides an initial reference for how much material must be removed from the piston crown. A more precise calculation of compression ratio will be carried out in Section 2, once the detailed geometry is finalized.

Figure 11: Drawings of the new piston head design.

During the piston design process, special attention was given to maintaining uniform wall thickness, especially in critical areas such as the region surrounding the cooling oil galleries and the center of the piston crown. This design strategy is crucial for ensuring sufficient thermal resistance and mechanical integrity under high-load and high-temperature operating conditions. These structural and thermal considerations will be further analyzed in the following section using FEA to validate the robustness of the piston geometry.

2.2 Compression Ratio Measurement

Having an accurate CAD model of the piston is essential for subsequent simulations, as it can significantly influence the behavior of the combustion model. Verifying the CR using this model allows for validation of the actual engine geometry, which is critical to ensure the accuracy of future simulations and performance predictions.
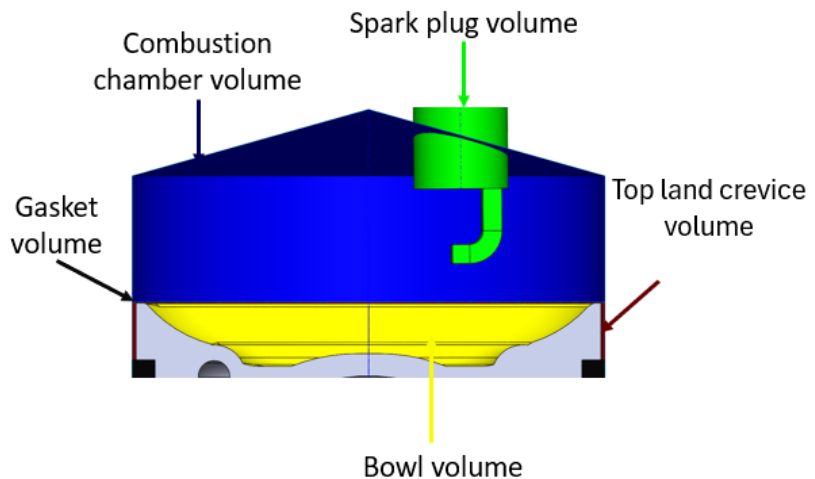
Figure 12: Volumes measured for CR calculations.

However, obtaining a highly precise CR is challenging due to numerous small geometric details within the engine, such as valve seat recesses, the squish effect of the head gasket when the cylinder head bolts are torqued, and the fact that a complete engine CAD model is not available. To achieve the highest possible accuracy, a hybrid approach is used, combining physical measurements with those derived from the CAD model (see *Figure 12*).

2.2.1 Volume Measured with CAD

Since the exact CAD model used to machine the piston head is available, it is possible to accurately measure the bowl volume using SolidWorks with a high degree of precision. The same approach applies to the calculation of the top-land crevice volume, as the required geometric parameters such as the piston diameter, cylinder bore, and crevice height are all known. These precise volume measurements are essential inputs for determining the engine's compression ratio and ensuring consistency between the CAD model and the physical component.

$$V_{top\ land\ crevice} = \text{thickness} * \pi * (\text{bore}^2 - \text{piston diameters}^2)/4 \quad (1)$$

$$V_{gasket} = \text{thickness} * \pi * \text{bore}^2/4 \quad\quad (2)$$

$$V_{bowl} = V_{flat} - V_{modified} \quad\quad (3)$$

Table 2: CAD and real measurements

Method	Location		Measurements	Uncertainty
Calipers	Piston diameters	[mm]	72.9	+/- 1.0E-01
Calipers	Cylinder bore	[mm]	73.7	+/- 1.0E-01
Calipers	Gasket thickness	[mm]	1.53	+/- 1.0E-02
Equ. 1	V_{gasket}	[cc]	6.53	+/- 4.6E-02
Calipers	Chamber Crevice Thickness	[mm]	9.0	+/- 1.0E-01
Equ. 2	$V_{top\ land\ crevice}$	[cc]	0.83	+/- 9.8E-03
CAD	V_{flat}	[cc]	121.1702	+/- 1.0E-04
CAD	$V_{modified}$	[cc]	96.57704	+/- 1.0E-04
Equ. 3	V_{bowl}	[cc]	24.6	+/- 1.4E-04

2.2.2   Volume Measured with Water Filling

For the remaining measurements since the full engine CAD model is not provided by Kohler Engines, a combination of experimental methods is used. The volumes of the cylinder head and spark plug cavity are measured using a liquid displacement method (e.g., water filling). To ensure transparency and improve the reliability of the compression ratio estimation, all associated measurement uncertainties are documented in the table *below*.

Table 3: Water filling measurements

Method	Location		Measurements	Uncertainty
Water	Spark Plug	[cc]	3.6	+/- 1.0E-01
Water	Combustion Chamber	[cc]	6.9	+/- 1.0E-01

2.2.3 Final Compression Ratio Calculations

The CR is defined as the ratio between the volume at Bottom Dead Center (BDC) and the volume at Top Dead Center (TDC). The TDC volume has already been determined by summing all previously calculated clearance volumes. To compute the BDC volume, the engine stroke is used to determine the swept volume of the cylinder.

$$V_{BDC} = V_{TDC} + \text{Stroke} * \pi * \text{bore}^2/4 \qquad (4)$$

$$CR = V_{BDC}/V_{TDC} \qquad (5)$$

Table 4: Compression ratio final calculation

Location		Measurements	Uncertainty
Spark plug	[cc]	3.6	+/- 1.0E-01
Gasket	[cc]	6.53	+/- 4.6E-02
Bowl	[cc]	24.6	+/- 1.4E-04
Combustion chambre	[cc]	6.9	+/- 1.0E-01
Top land crevice	[cc]	0.83	+/- 9.8E-03
Stroke	[mm]	324	+/- 9.7E-03
Volume TDC	[cc]	35.2	+/- 1.5E-01
Volume BDC	[cc]	359	+/- 1.9E-00
CR+	[-]	10.26	
CR	[-]	10.19	+/- 6.8E-02
CR-	[-]	10.12	

With an estimated uncertainty of ±0.07, the compression ratio is calculated to be approximately 10.2:1. It is important to note that the measurement of the combustion chamber volume obtained via liquid displacement may introduce a slight margin of error due to factors such as surface tension, air bubbles, or imperfect sealing. Nonetheless, the overall result provides a reliable estimate for use in simulation and design validation.

2.3 Finite Elements Analysis Validation

Since the new design involves removal of material from the OEM piston, it is essential to perform a FEA before any physical testing is conducted. Additionally, because the piston crown is in direct contact with the combustion gases, it is subjected to elevated temperatures throughout each combustion cycle. Therefore, the first step is to conduct a thermal analysis to evaluate how the piston material responds to high temperatures. This is followed by a structural stress analysis, which is coupled with the thermal results to assess deformation and determine whether the redesigned piston may be prone to mechanical failure under operating conditions.

2.3.1   Analysis of the Piston Material

The OEM piston is made from cast aluminum alloy AlSi12, one of the most used materials in industrial piston applications due to its favorable strength-to-weight ratio and thermal properties. All mechanical and thermal properties used in the simulation are based on validated material data from The Aluminum Automotive Manual [6]. For the thermo-mechanical coupled analysis, the two most critical material properties are the Young's modulus and Poisson's ratio. Since the piston operates under high-temperature conditions, it is essential to account for the temperature dependence of these properties. In the Table 5, The Aluminum Automotive Manual reports experimental data of Young's modulus and Poisson's ratio for this specific cast aluminum alloy AlSi12.

Table 5: Experimental values from F. Rösch: Physical properties of piston alloys

Modulus of elasticity [MPa]	Poisson's ratio [-]	Temperature [K]
80000	0.33	273.15
77500	0.33	373.15
74000	0.33	473.15
70000	0.34	573.15
65000	0.36	673.15
59000	0.39	773.15
56000	0.41	823.15

Using the Ordinary Least Squares method (OLS) by minimizing the Sum of the Squared Residuals (SSR), the discrete experimental values of the material properties can be interpolated into continuous functions of temperature. This approach enables the generation of smooth temperature-dependent curves for both Young's modulus and Poisson's ratio. These continuous functions are then used in the thermal analysis, providing a more accurate temperature field.
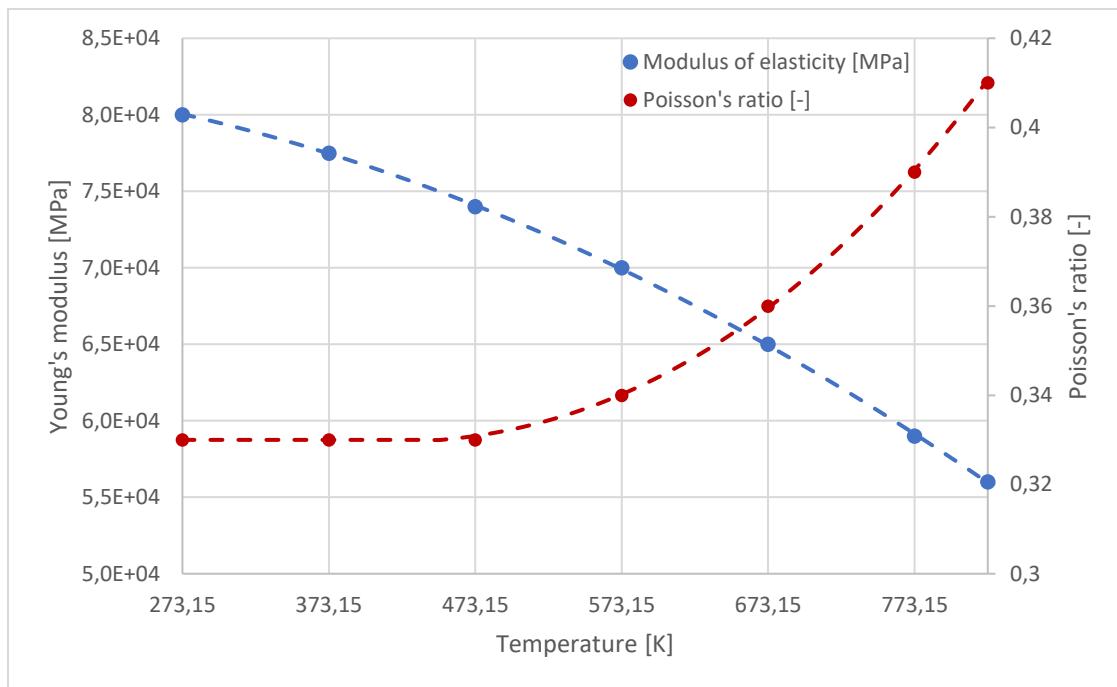

Figure 13: Interpolated mechanical properties of AlSi12 as a function of the Temperature.

The OLS method is also applied to interpolate the Ultimate Tensile Strength (UTS) of the AlSi12 alloy as a function of temperature. However, in this case, special attention is given to include uncertainty analysis. Since the UTS will be used in the final stage of the study to calculate the safety factor, it is essential to account for variability in the material properties. Incorporating this uncertainty ensures coherence throughout the analysis and provides a more realistic and reliable assessment of the structural integrity of the redesigned piston under thermal and mechanical loading.
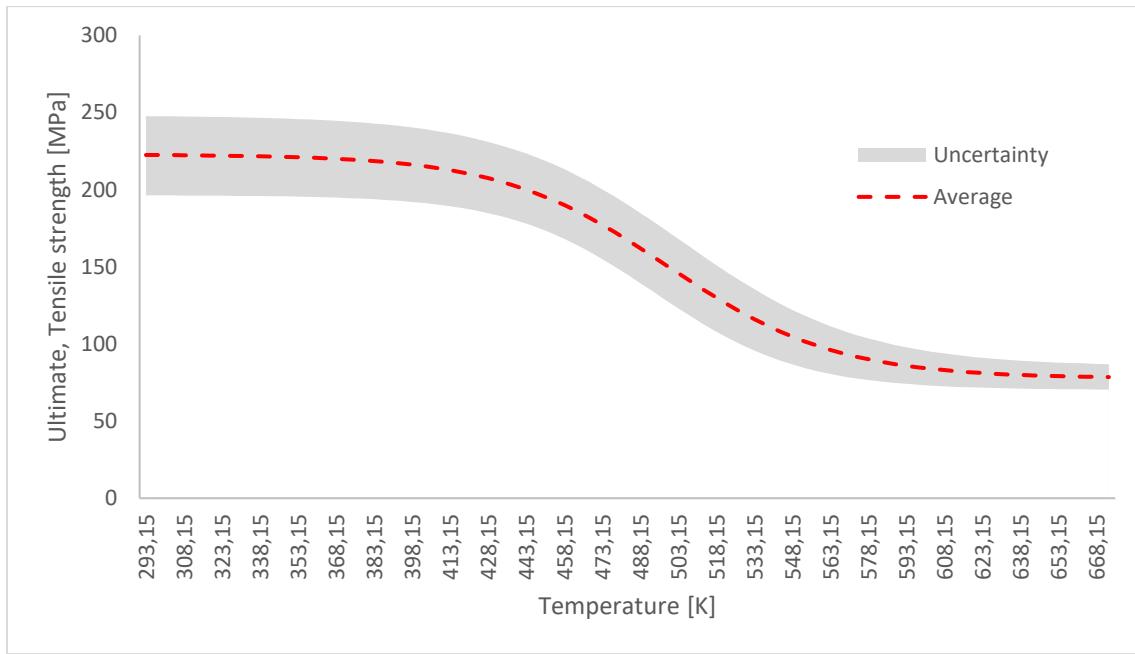
Figure 14: Interpolated UTS of AlSi12 as a function of the Temperature.

For simplified thermal simulations in the FEA software CAE Abaqus, the following thermal material properties are required: thermal conductivity, specific heat capacity, and thermal expansion coefficient. These values were obtained from the same source as the mechanical properties: F. Rösch, Physical Properties of Piston Alloys [6]. Those values are constant and don't need the same interpolation as the previous mechanical properties.

21

Table 6:Thermal properties of AlSi12 by F. Rösch: Physical properties of piston alloys

Properties		Values
Thermal Conductivity	[W/m.K]	138
Specific Heat Capacity	[J/g.°C]	0.850
Melting Point	[°C]	550

2.3.2   Thermal FEA Simulation

To ensure that the FEA thermal simulation accurately represents the actual heat transfer occurring within the piston, experimental thermal data were used to define the boundary conditions. These temperature measurements, obtained from a piston of similar geometry and operating conditions, were sourced from Internal Combustion Engine Fundamentals by John B. Heywood [7]. This reference provides realistic estimates of the temperature distribution across key regions of the piston, including the crown, skirt, and ring belt (see *Figure 15*).
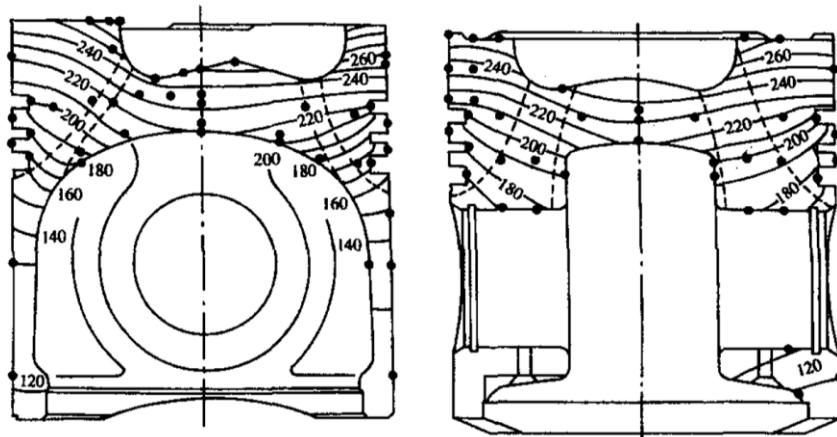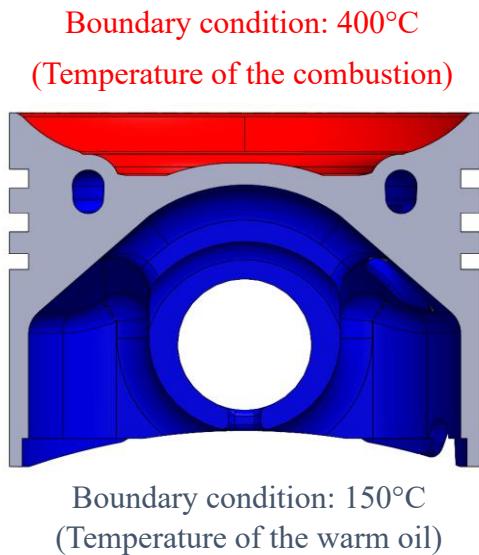

Figure 15: Temperature [°C] distribution across an operating H2 piston.

To closely replicate the thermal conditions reported in the *Figure 15*, the temperature boundary conditions were divided into two distinct regions, as illustrated in the figure *below*. The first region corresponds to the top of the piston, which is in direct contact with the hot combustion gases, with an imposed temperature of approximately 400 °C, typical for hydrogen combustion. The second region represents the portion of the piston in contact with the cooling oil, where temperatures generally stabilize around 150 °C once the engine reaches operating temperature. Although the engine under study is not expected to reach these exact temperatures during normal operation, these values were chosen to represent a worst-case thermal scenario for the analysis.

Boundary condition: 400°C
(Temperature of the combustion)

Boundary condition: 150°C
(Temperature of the warm oil)

Figure 16: Boundary conditions for thermal analysis.

The simulations were performed using Abaqus CAE, employing the steady-state heat transfer model. A tetrahedral mesh with an element size of 2 mm was used to discretize the piston geometry. The results of this initial thermal analysis for both the OEM piston and the new design are presented *below*.
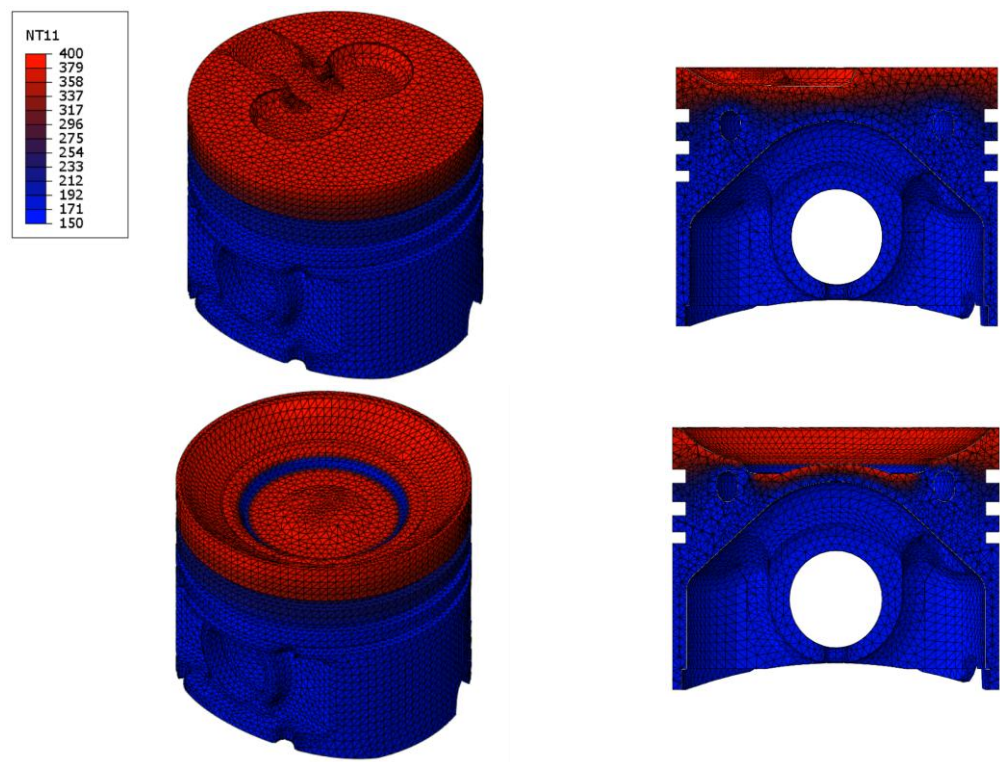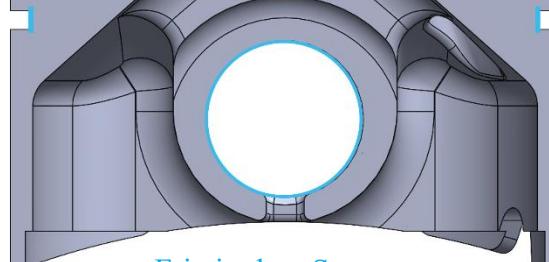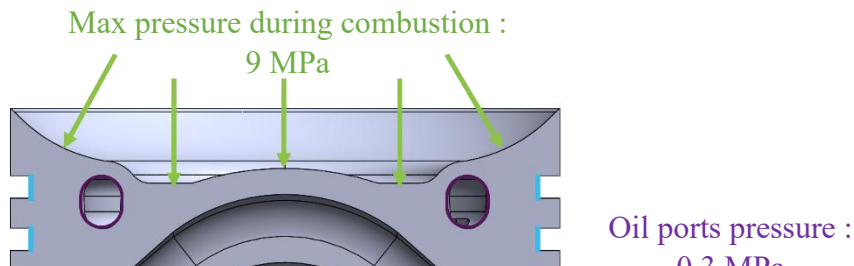
Figure 17: Results of the thermal simulation on Abaqus [°C].

2.3.3 Stress/Thermal FEA Simulation

The FEA stress analysis was conducted using the results of the thermal simulation as input to account for temperature-induced stresses. Additionally, specific assumptions were made regarding the boundary conditions to accurately represent the piston's mechanical constraints. Since a key aspect of this analysis is to determine whether deformation could lead to contact between the piston head and the cylinder wall, the boundary conditions were applied at the location of the piston rings rather than on the piston skirt. The initial simulation was performed by applying a pressure load of 9 MPa on the piston crown, combined with the boundary conditions *below*:

Figure 18: Boundary conditions for structural stress analysis.

For the stress analysis, Abaqus CAE was employed using Static, General solver with the same 2 mm tetrahedral mesh as in thermal simulations. This setup allowed the direct incorporation of the thermal results as input for the coupled thermo-mechanical analysis. This initial simulation represents a worst-case scenario, aimed at determining whether the piston deformation causes contact between the piston crown and the cylinder wall (see *below*).
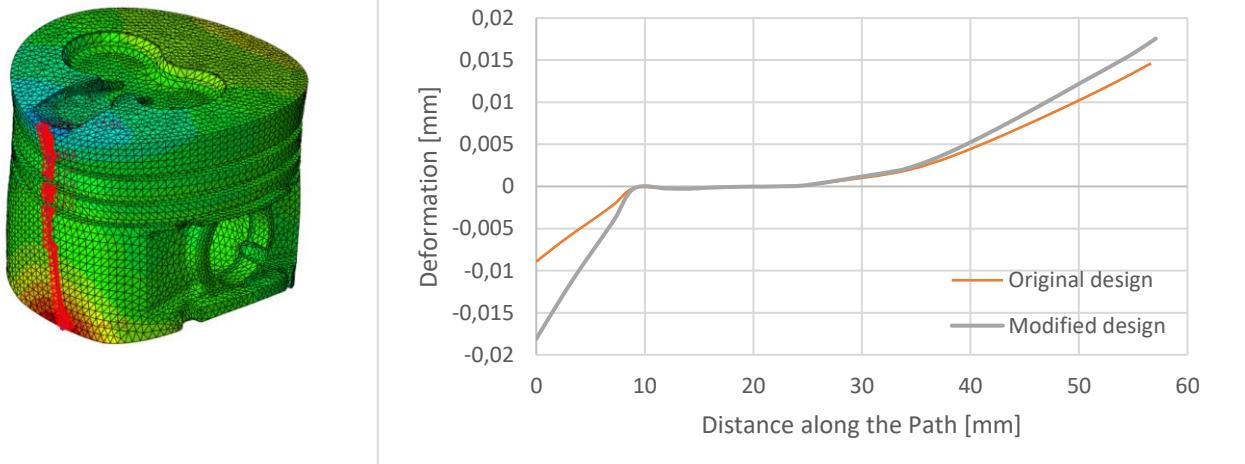
Figure 19: Comparison of the deformation Vs. distance along the red path (figure on the left).

Although the modified piston design exhibits slightly increased deformation, the difference is not significant enough to risk contact between the piston and the cylinder wall. This is confirmed by the fact that the maximum allowable cold deformation is 0.7 mm, as indicated in the table *below*

Table 7: FEA Simulations result on the deformations

Design		OEM	Modified
Max deformation	[mm]	0.009	0.018
Max deformation allowed	[mm]	0.7	
Clearance Piston/Cylinder	[mm]	0.691	0.682

Since the peak cylinder pressure is not yet known, a parametric sweep was conducted by applying different pressure values to both the OEM and modified piston designs. Using the material properties and resulting stress distributions, the safety factor was calculated for each case to enable a comparative assessment of structural integrity.
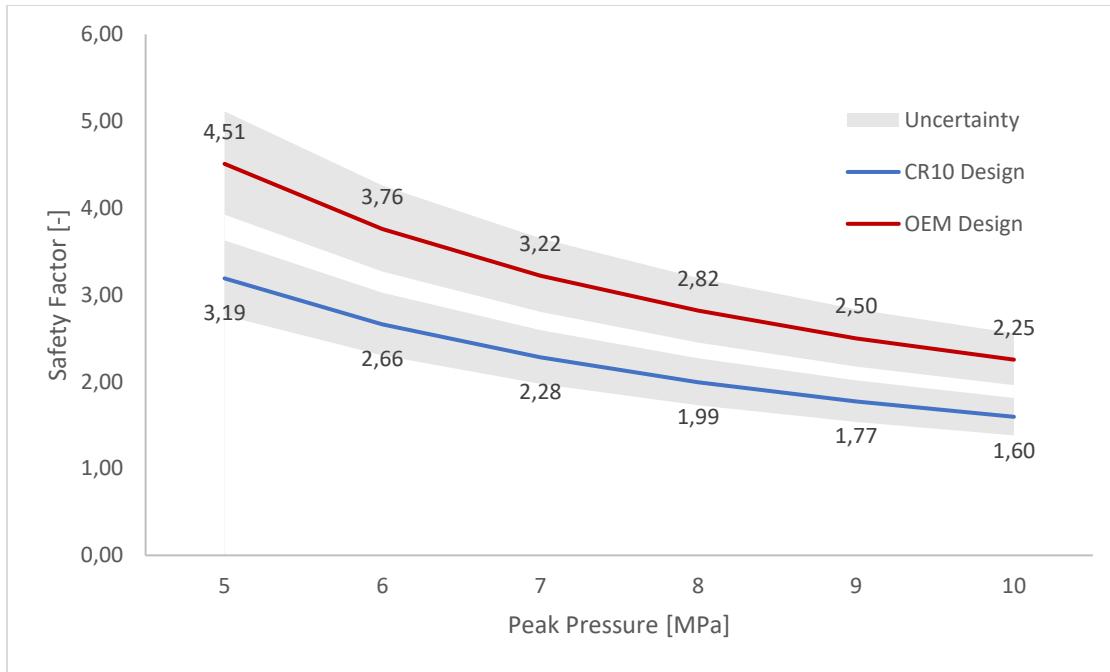
Figure 20: Comparison of Safety Factor (SF) for different Peak Pressure values.

The OEM piston was originally designed to withstand a peak cylinder pressure of 10 MPa, consistent with its high compression ratio of 28:1 and operation on diesel fuel. To ensure a conservative level of safety, a target safety factor (SF) of approximately 2.25 is recommended, based on the premise that the OEM design can reliably handle this pressure. *Figure 20* illustrates that, to maintain this safety factor, the peak cylinder pressure should not exceed 7 MPa. However, since the modified piston operates with a significantly lower compression ratio, the resulting peak pressure is expected to be considerably reduced. Therefore, maintaining a design with a slightly lower SF of around 2 remains acceptable, especially given the reduced mechanical loading.

27

3. H2 COMBUSTION SIMULATION

3.1 Workflow Overview

After completing the engine design for conversion to a hydrogen PFI engine, the focus shifts to simulation. Due to the absence of experimental engine testing, the objective of this section is to develop a fully predictive simulation model based solely on the engine geometry outlined in the previous section 2.1.1, and a predictive combustion model.

Typically, calibrating a 1D/0D model in GT-Power involves using the SI Turb combustion model, which requires a Three-Pressure Analysis (TPA) [8]. This process relies on real measurements of intake, in-cylinder, and exhaust pressures. To bypass the need for experimental calibration, a CFD simulation is employed to generate an accurate combustion model. Since CFD provides a 3D solution, the Species Mass Fraction (SMF) is extracted and converted into a Mass Fraction Burned (MFB) curve, which is then used as input for the 1D simulation in GT-Power.
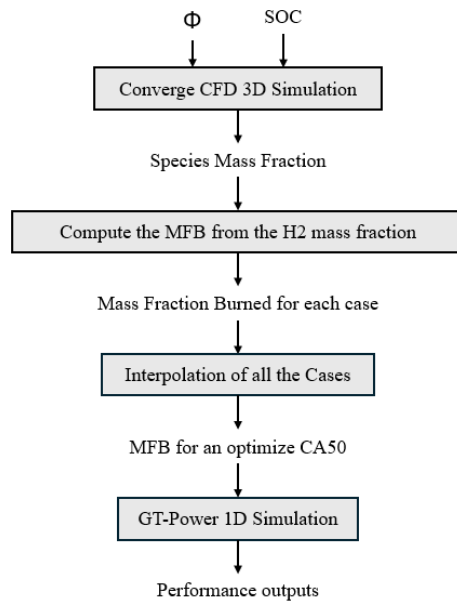

Figure 21: Diagram of the predictive model workflow.

To keep the simulations manageable, given their high computational cost, the focus is placed on two parameters that have a direct impact on engine performance and are known to be easily adjustable during engine testing: the equivalence ratio (Φ) and spark timing or also known as Start of Combustion (SOC). It is assumed that the engine operates within a narrow RPM range, such that its influence on combustion and performance is negligible. The same assumption applies to intake pressure and temperature, which will be discussed in more detail in the *Configuring Boundaries* Conditions section. For a better understanding, Φ can be defined with the Air-to-Fuel Ratio (AFR) or with lambda. For hydrogen, the stoichiometric AFR is 34:1 by mass:

$$\Phi = AFR_{sto}/AFR \qquad (6)$$

$$\Phi = 1/\lambda \qquad (7)$$

An engine is considered fuel rich when $\Phi > 1$ and fuel lean when $\Phi < 1$.

A set of simulations, comprising various combinations of Φ and SOC, is performed using CONVERGE CFD (Convergent Science, Inc.). The results are then interpolated to generate a fully defined map of combustion behavior. Knowing that the engine achieves maximum efficiency at a constant CA50, all MFB curves corresponding to this optimized CA50 are exported to GT-Power (GAMMA Technologies) to assess the final performance of the optimized engine.

3.2 3D CFD Simulations

3.2.1   3D Mesh of the Engine Cylinder

The first step in the CFD simulation process is to obtain an accurate CAD model of the piston and cylinder head. For this purpose, the same CAD model previously developed for the CR measurement section 2.1.3 was reused. This ensures a highly accurate geometry, consistent with the actual CR and including a detailed representation of the spark plug electrodes. Particular attention is given to this region, as it represents the ignition source and is thus critical to the accuracy of the combustion simulation. The cylinder CAD model is exported from SolidWorks to CONVERGE Studio for meshing. The model is then cleaned following the official CONVERGE CFD preprocessing workflow [4], ensuring that there are no intersections, open edges, non-manifold geometries, incorrect surface normals, or overlapping triangles.
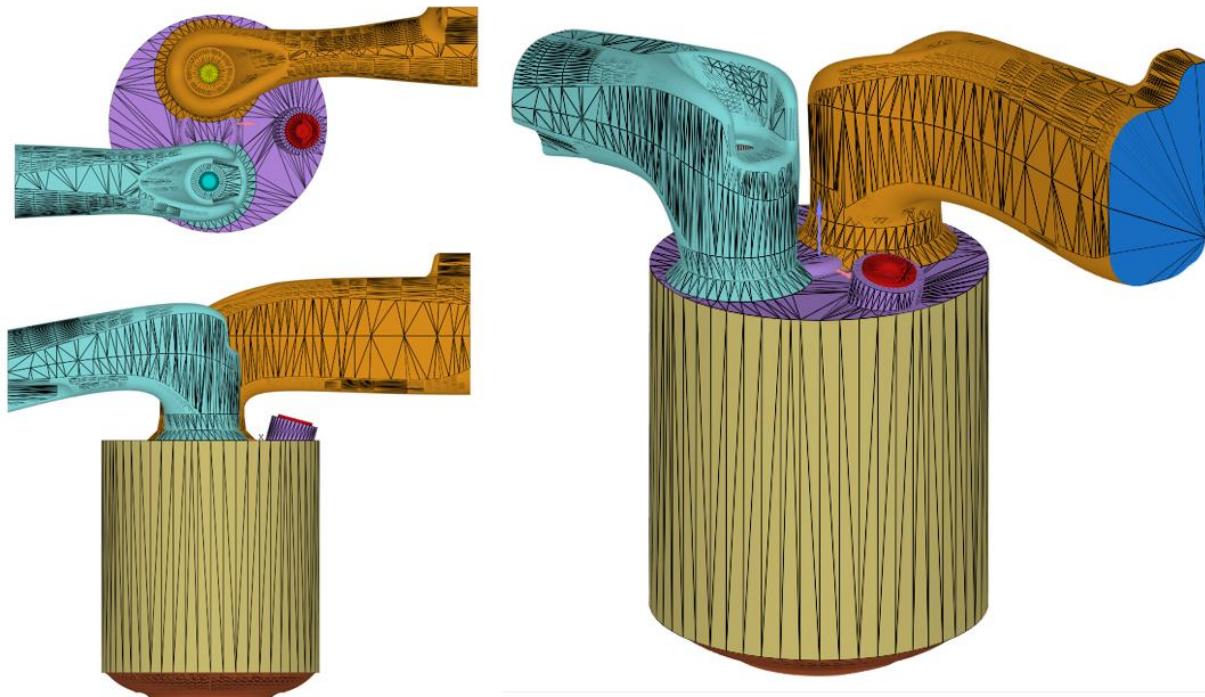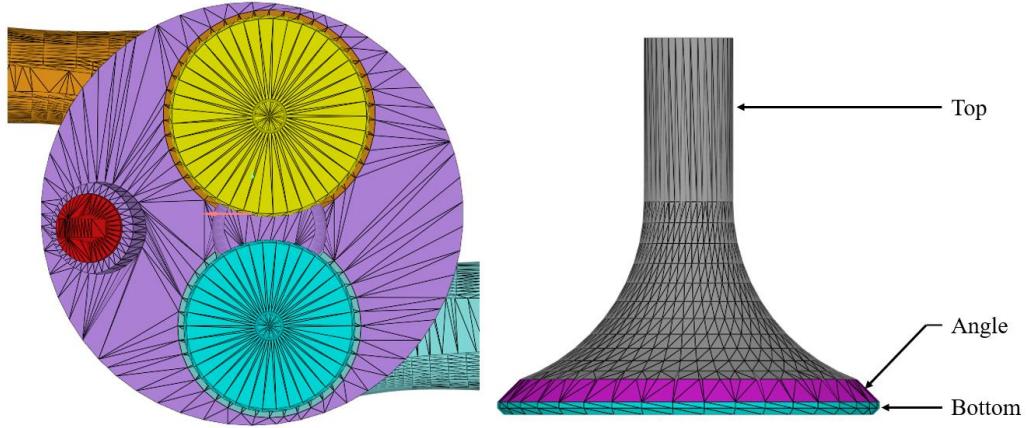

Figure 22: Mesh of the full cylinder used for the CFD simulations.

After cleaning the mesh, it is essential to ensure that each region of the geometry is properly flagged. This step is critical to maintaining consistent boundary definitions and ensuring that grid refinement is applied accurately. For example, special attention is required near the intake and exhaust valves, as well as the valve seats. These areas must be subdivided into three distinct regions, valve top, valve angle, and valve bottom, facilitate mesh generation and enable the use of Adaptive Mesh Refinement (AMR), a native feature of CONVERGE CFD that dynamically adjusts mesh resolution based on flow features. The same level of detail is applied to the spark plug electrode to ensure accurate simulation of ignition and early flame development.

Figure 23: Details of the heads and valve mesh.

The final surface mesh consists of 41,072 triangles and 61,608 edges, resulting in a relatively simple model, intentionally designed to reduce computational cost. However, localized refinement is necessary around the intake and exhaust valve seats. In these regions, the high flow rates during valve opening and closing lead CONVERGE CFD to automatically subdivide the mesh to maintain numerical stability. This increases computational time slightly during each simulation step.

Grid control is a critical phase of the setup, as it directly determines the spatial resolution and accuracy of the simulation. This step can be time-consuming, requiring several iterations of mesh refinement to ensure sufficient resolution in key areas, such as the ignition site, to accurately capture phenomena like early flame development or knock. Fortunately, the AMR feature in CONVERGE CFD proves to be highly effective. It allows for a fine mesh at the flame front during combustion, while maintaining a coarser mesh during the intake and exhaust strokes, significantly reducing overall computational demand without compromising accuracy. The base grid size is 0.004m and SGS represents the Sub-Grid Scale which the number of divisions to the base grid size:

Table 8: Grid control details with embedding and AMR settings

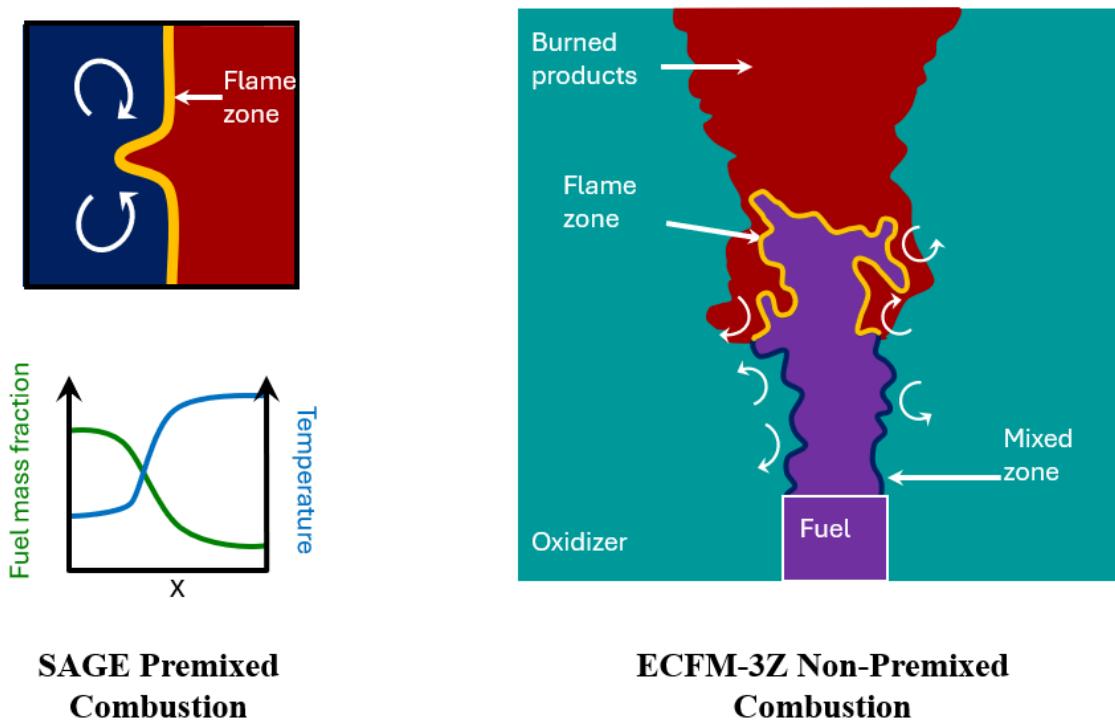| Type	Location	Criterion	SGS	Grid size
Embedding	Cylinder Chamber, intake & exhaust	Permanent	2	2mm
	Spark plug electrode	Permanent	6	0.67mm
	Exhaust valve angle	Permanent	3	1.3mm
	Intake valve angle	Permanent	3	1.3mm
AMR	Cylinder	Velocity	3	Minimum 1.3mm
	Cylinder	Temperature	4	Minimum 1mm
	Intake	Velocity	3	Minimum 1.3mm

3.2.2 CONVERGE CFD Simulation Setup

Once the mesh model is validated in CONVERGE Studio, the remaining simulation setup can be completed. To simplify this process, CONVERGE CFD provides a pre-configured setup for hydrogen DI engines. Although a few modifications are required to adapt this setup to the specific case of PFI, the default configuration includes combustion and turbulence models that are already well-tuned for hydrogen combustion. This significantly streamlines the process, as the baseline parameters have been optimized for accurate and stable simulation of hydrogen fueled engines.

The first element of the simulation setup is the reaction mechanism. To maintain a balance between model simplicity and chemical accuracy, the C3Mech V3.3 mechanism was selected [9]. This mechanism, developed by the Computational Chemistry Consortium (C3), is widely used in CFD applications and is considered a standard for combustion simulations. It includes 3,761 chemical species and 16,522 reactions, providing a comprehensive representation of combustion chemistry. Since the simulation focuses on the combustion of pure hydrogen, only a subset of this extensive mechanism is actively involved in the reaction process. The relevant portion of the mechanism used for hydrogen oxidation is detailed *below*:

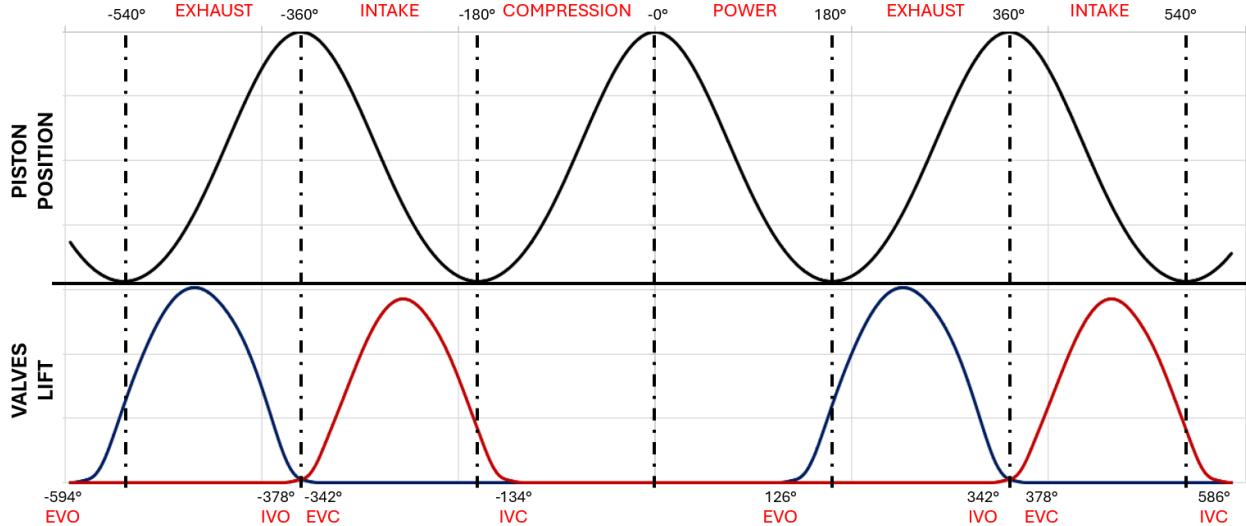*Table 9: C3Mech V3.3 mechanism filtered for H2 combustion.*

Number of available elements	6	C H O N HE AR
Number of available species	12	AR N2 HE H2 H O2 O H2O OH OHV H2O2 HO2
Number of available reactions	37	-

The second major setting in the simulation concerns combustion modeling, which governs how the fuel–air mixture behaves and how the flame propagates within the combustion chamber. The default configuration in CONVERGE CFD uses a combination of ECFM-3Z (Extended Coherent Flame Model, three zones) and the G-equation model. This method categorizes the mixture into three regions, burned, on-flame, and unburned, and provides a computationally efficient approach based on empirical data. However, since this model has been primarily validated for conventional hydrocarbon fuels, it is less suitable for hydrogen combustion. Instead, a more general and physically accurate approach is adopted by using the SAGE detailed chemistry solver. SAGE enables the use of full chemical kinetics, and when coupled with adaptive zoning, it can capture complex phenomena such as autoignition and knock, which are critical for hydrogen engine simulations (see *Figure 24*).

SAGE Premixed Combustion

ECFM-3Z Non-Premixed Combustion

Figure 24: CONVERGE CFD differences between Premixed and Non-Premixed combustion models [4].

For turbulence modeling, the high reactivity of hydrogen and the relatively small engine volume make Direct Numerical Simulation (DNS) unnecessary. Instead, a simpler and computationally efficient Reynolds-Averaged Navier–Stokes (RANS) model is sufficient to capture the dominant flow features, such as macroscopic vortices and swirl. Specifically, the RNG k–ε model is recommended by CONVERGE CFD for PFI hydrogen ICEs. Additionally, since the injection is not modeled as a spray event, parcel-based injection modeling is omitted from the simulation setup.

Figure 25: Engine simulations Events.

Finally, the simulation timing and valve event parameters (IVO, IVC, EVO, EVC) were defined based on the real engine's specifications. To ensure that the simulation captures steady-state engine behavior, a total of two full engine cycles (1,440 crank angle degrees) is simulated. This allows for accurate prediction of residual gas effects during the second combustion event, as well as the evaluation of any engine incomplete combustion.

3.2.3 Configuring Boundaries Conditions

For the boundary conditions in the simulation, the fully predictive nature of the model prevents the use of experimentally measured intake and exhaust pressures and temperatures. To address this limitation, a preliminary GT-Power 1D model of the complete intake and exhaust systems was developed. This simplified model provides initial estimates of the airflow characteristics through the intake system, as well as the pressure and temperature of the exhaust gases. Although this approach does not yield fully accurate values, it offers a reasonable starting point for defining boundary conditions in the CFD simulation. These initial estimates enable the setup of realistic operating conditions in CONVERGE CFD and support the goal of creating a predictive model in the absence of experimental data.
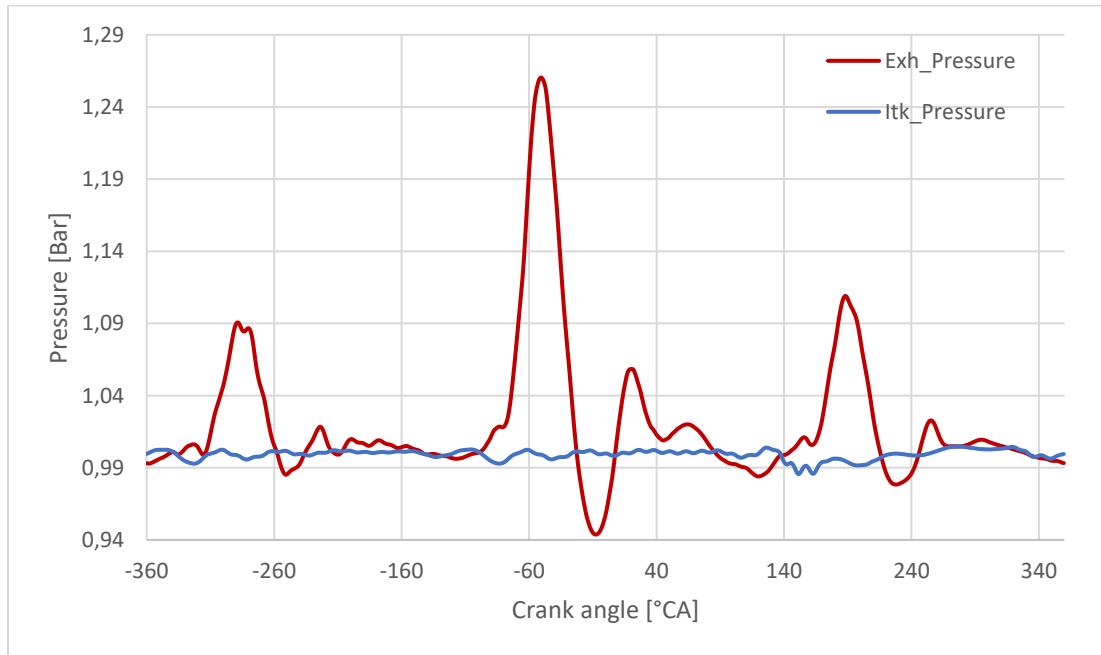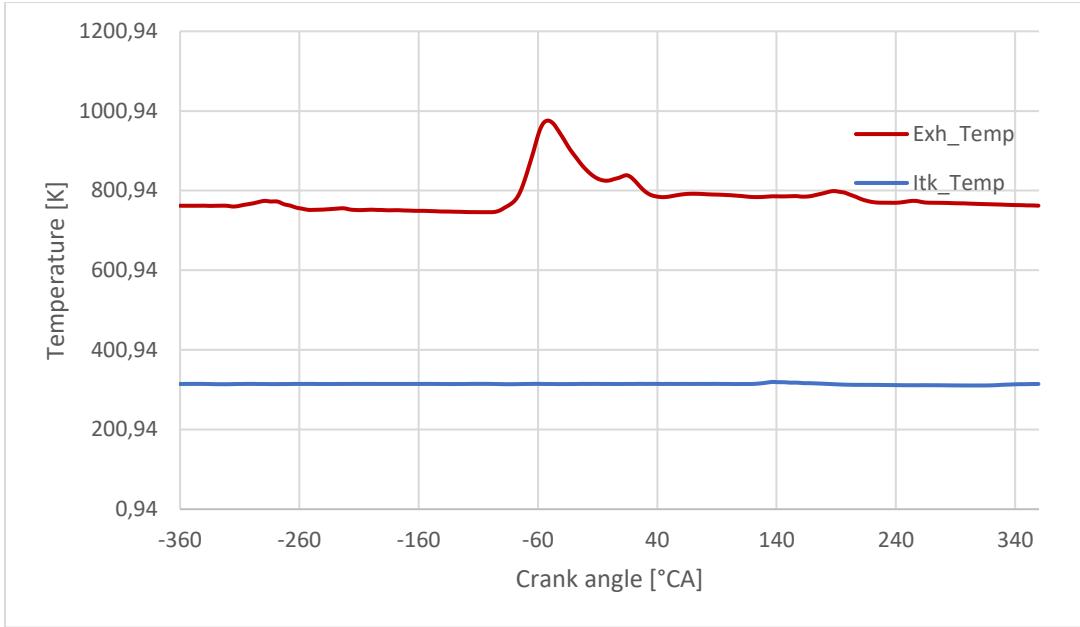

Figure 26: Pressure Vs. CA at the intake and exhaust boundaries.

Figure 27: Temperature Vs. CA at the intake and exhaust boundaries.

To control the equivalence ratio in the simulation, the injectors are not explicitly modeled. Instead, a premixed inflow of air and pure hydrogen is introduced directly at the intake boundary. This simplification is justified by the fact that, in a PFI configuration, the injectors are located far upstream from the flow inlet defined in the CFD model. As a result, the fuel–air mixture is assumed to be fully mixed before entering the computational domain. The air–fuel mixture composition at the inlet can then be calculated based on the desired ϕ and the stoichiometric air-to-fuel ratio of hydrogen. Using this value, the required mass or molar fractions of air and fuel in the mixture can be determined as follows:

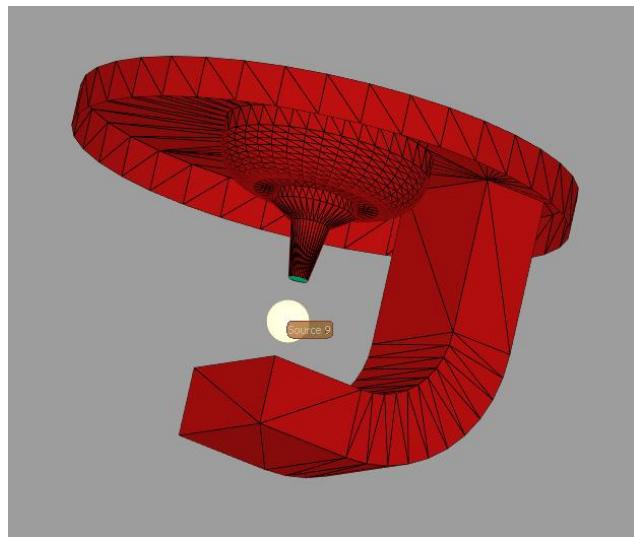$$Air_\% = \frac{100}{1+\frac{\phi}{AFR_{sto}}} \qquad (8)$$

$$Fuel_\% = 100 - Air_\% \qquad (9)$$

Then, knowing that air is composed of 76.7% nitrogen (N_2) and 23.3% oxygen (O_2), and that the fuel is pure hydrogen (H_2), we can calculate the species composition of the premixed mixture at the inflow boundary based on the previous AFR and ϕ calculations (see *below*).

Table 10: Percentage of each species at the intake based on equivalence ratio.
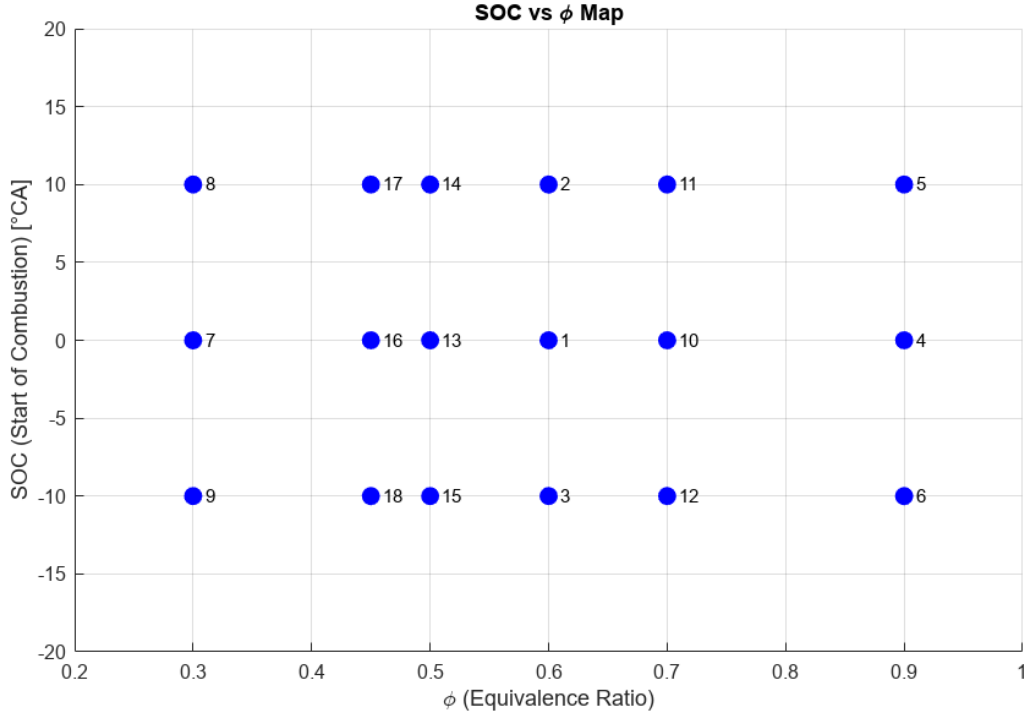
ϕ	H_2	N_2	O_2
0.3	0.87%	76.03%	23.10%
0.4	1.16%	75.81%	23.03%
0.45	1.31%	75.70%	23.00%
0.5	1.45%	75.59%	22.96%
0.6	1.73%	75.37%	22.90%
0.7	2.02%	75.15%	22.83%
0.9	2.58%	74.72%	22.70%

To control the SOC, an energy source is placed near the spark plug electrode. Ignition is a particularly complex aspect to model accurately. Therefore, instead of replicating the exact behavior of a real spark plug, the recommended values provided by CONVERGE Science are used: 20mJ of energy released over 0.5° CA, followed by an additional 20mJ over 10° CA.

Figure 28:Converge CFD spark plug details and energy source.

Each simulation case is defined by two parameters: ϕ and SOC. Multiple cases were created according to the 2D Map presented *below*. Each point on the 2D map represents a specific case; for example, Case 1 corresponds to an equivalence ratio of 0.6 and a spark timing of 0° CA.

Figure 29: 2D Map showing the combinations of SOC and ϕ tested for each case

The approach used to generate this map involved an initial SOC sweep at a selected ϕ known to perform well based on previous studies and existing data on hydrogen combustion [5]. Additional sweeps were then conducted at the extremes of the operating range to spot knock, followed by refinement in regions where the results required greater resolution.

3.2.4 3D CFD Simulations Results

The simulation job is exported from CONVERGE Studio and submitted to the HPC cluster for execution. Given the HPC specifications, approximately 40 cores per node, a simulation spanning two engine cycles typically requires about one day to complete. Additionally, three to four simulations can be run in parallel, allowing for efficient batch processing.

After completion, the combustion behavior can be analyzed using Tecplot for CONVERGE. This post-processing step allows verification that the specified input parameters, the ϕ and SOC, have been correctly applied. The 3D visualization in Tecplot is particularly useful for identifying potential knock events and for detecting the presence of unburned fuel within the combustion chamber. This can be assessed by examining temperature contours.

Crank : 4.56
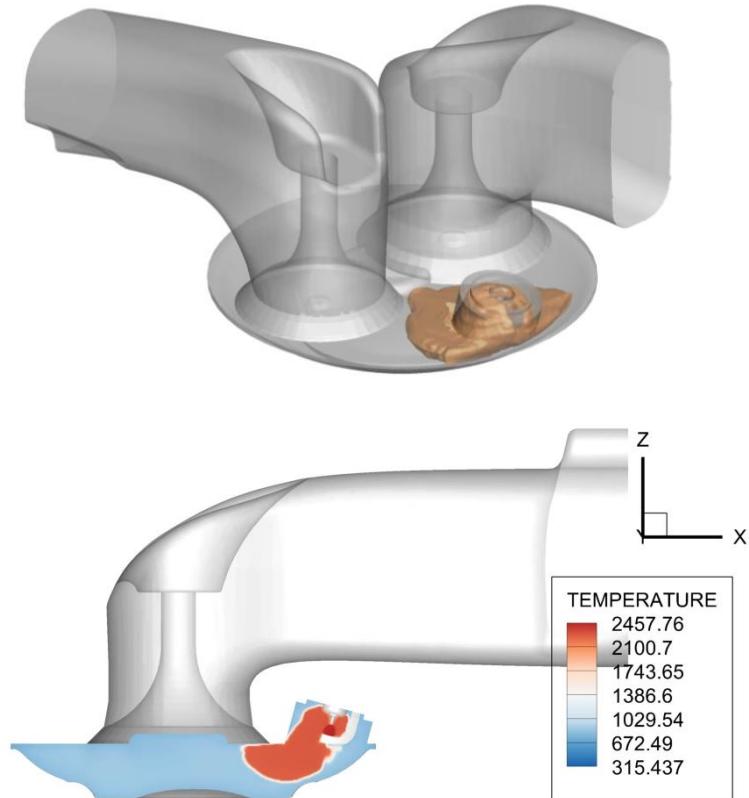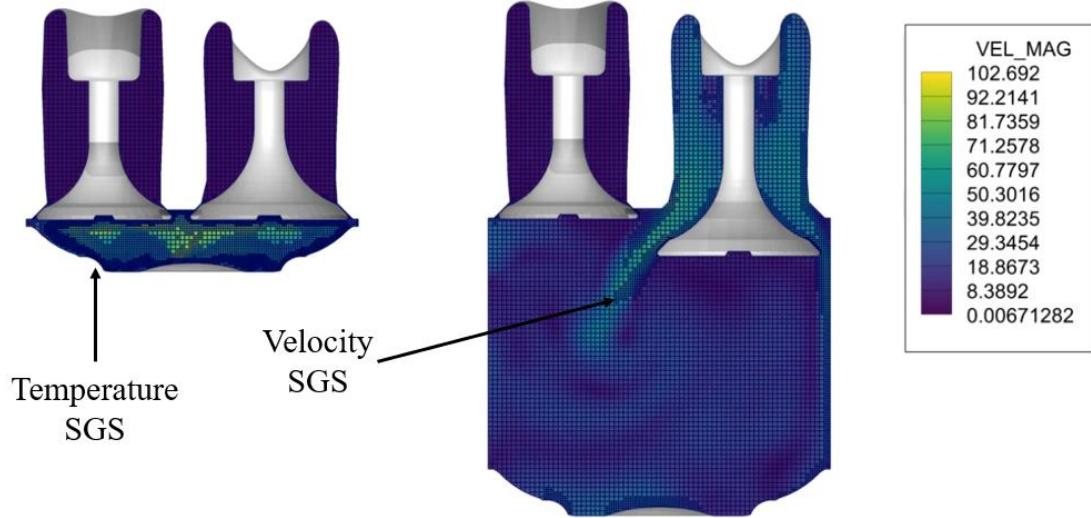
Figure 30: Temperature contour on Tecplot showing the development of the flame front.

40

This visualization is also valuable for evaluating the behavior of the AMR and verifying whether sufficient refinement levels have been applied in the grid control settings.

Figure 31: Adaptive Mesh Refinement.

By comparing the different cases, it becomes clear how spark timing affects the in-cylinder pressure during combustion. When ignition occurs around $-10°$ CA, the piston has not yet reached TDC, resulting in lower cylinder pressure and slower flame propagation. In contrast, ignition at TDC ($0°$ CA) corresponds to peak cylinder pressure, which significantly accelerates flame propagation.

The same principle applies to the equivalence ratio. A higher equivalence ratio ($\phi \approx 0.9$) results in a more reactive mixture, leading to faster combustion. However, this also increases the likelihood of knock occurrence. To quantify the flame propagation rate, the species mass fraction is used as a marker. The analysis is focused within the 700° CA to 850° CA range to isolate the second combustion cycle, specifically between Intake Valve Closing (IVC) and Exhaust Valve Opening (EVO). This step also serves to verify species conservation by examining the total mass fraction of all tracked species throughout the combustion event.
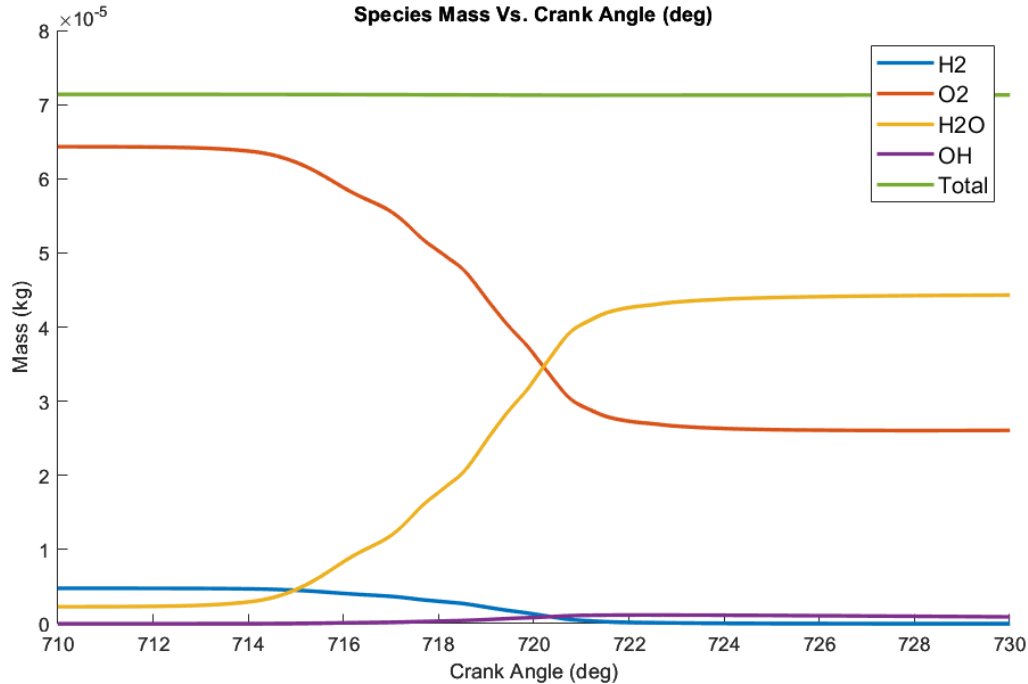

Figure 32: Species Mass Vs. CA for case 3 (ϕ=0.6 ; SOC = -10° CA).

3.3 3D to 1D Conversion

3.3.1 The MFB Curve

In CONVERGE Studio, the SMF data is exported and processed using a MATLAB script to generate the MFB curve. The calculation is straightforward: the MFB at any given crank angle is defined as the ratio of the mass of hydrogen (H_2) burned up to that point to the initial mass of H_2 present in the cylinder prior to ignition.

$$MFB(\theta) = \frac{mass_{H2,initial} - mass_{H2}(\theta)}{mass_{H2,initial}} \qquad (10)$$

For each combination of ϕ and SOC, an individual MFB curve is generated. To ensure compatibility with the GT-Power environment, a preprocessing step is applied in MATLAB. First, the MFB curves are interpolated to guarantee that they are monotonically increasing, as required for physical consistency. Then, all curves are resampled to contain exactly 1,000 data points, which is the maximum number accepted by GT-Power for MFB input profiles.
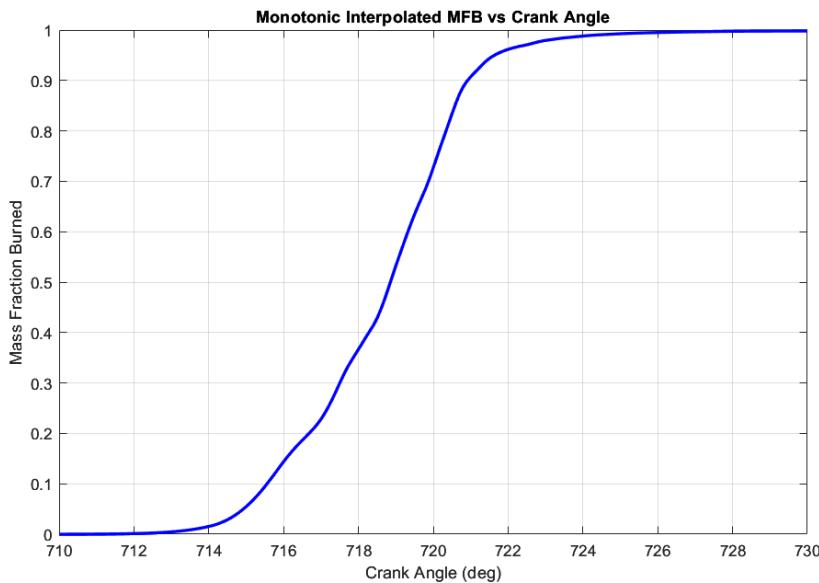

Figure 33: MFB Vs. CA for case 3 (ϕ=0.6 ; SOC = -10° CA).

At this stage, the most accurate MFB curves possible have been obtained for each simulation case. As a result, no approximation using a Wiebe function single or double is applied. This decision is justified by the fact that certain combustion characteristics, which are closely linked to specific aspects of the engine design (such as the presence of a pre-combustion chamber), introduce detailed features in the MFB curves that cannot be captured by simplified models. These features are often visible as small oscillations at the beginning of the MFB curve. Despite their subtle appearance, they have a measurable impact on the Heat Release Rate (HRR) and, consequently, on the overall performance of the engine. Those oscillations correspond to the flame expanding in a prechamber before the full cylinder.
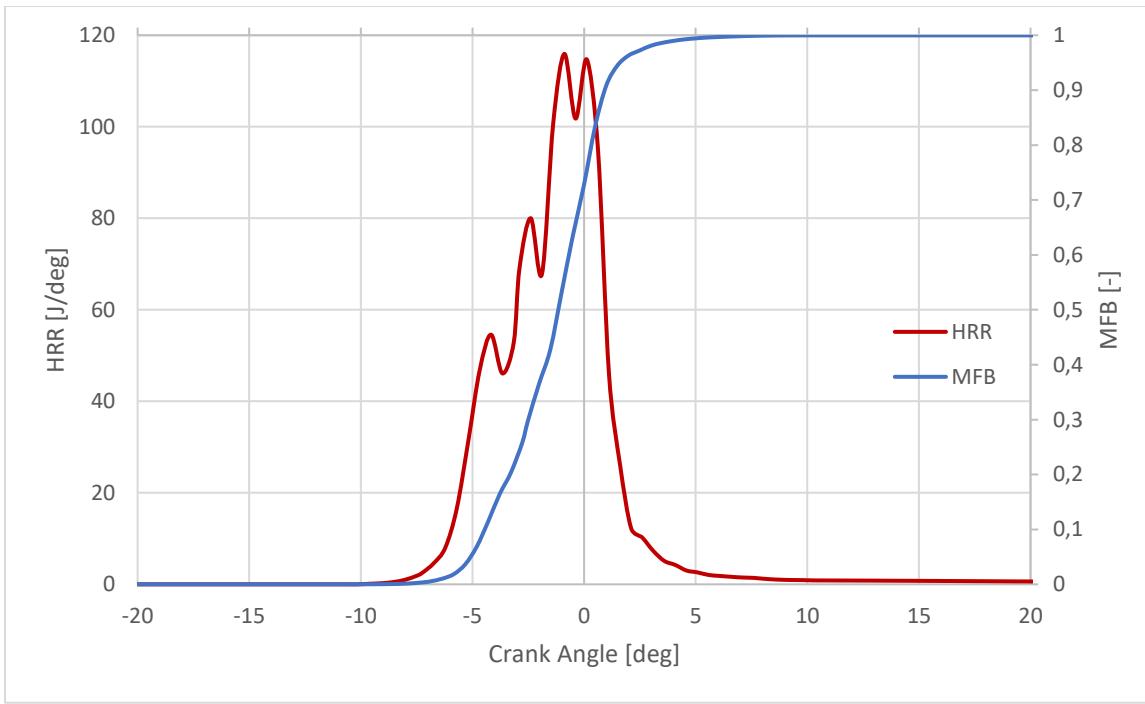
Figure 34: MFB and HRR Vs. CA for case 3 (ϕ=0.6 ; SOC = -10° CA) showing the impact of the oscillation's details importance on the HRR.

3.3.2 Interpolation of the MFB Curves on a 2D Map

Once MFB curves have been obtained for all cases, interpolation can be performed to generate continuous MFB curves at fixed values of either SOC or φ. Specifically, for a constant SOC, the MFB curves are interpolated across different equivalence ratios to obtain a continuous set of combustion profiles.

Figure 35: Example of interpolation on the equivalence ratios (φ=0.64) for a fixed SOC=0° CA.

Similarly, for a fixed equivalence ratio, MFB curves are interpolated across varying SOC values to provide a continuous combustion map as a function of spark timing.
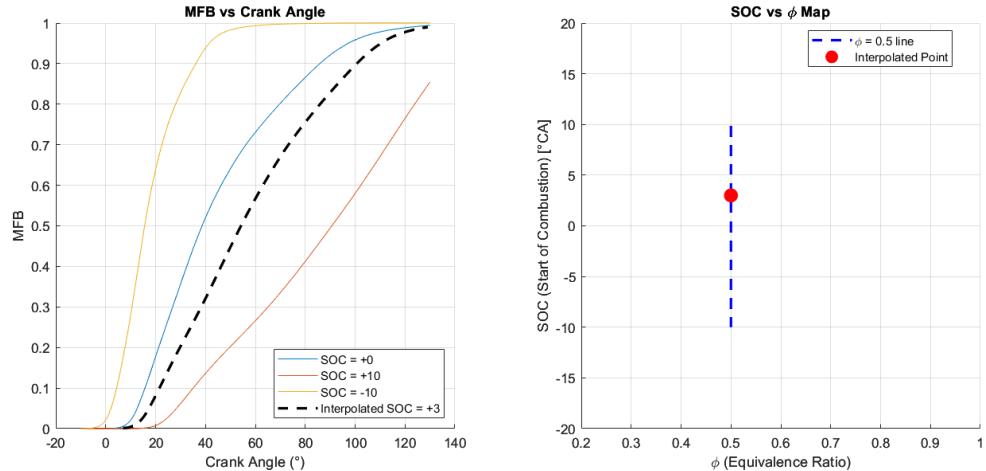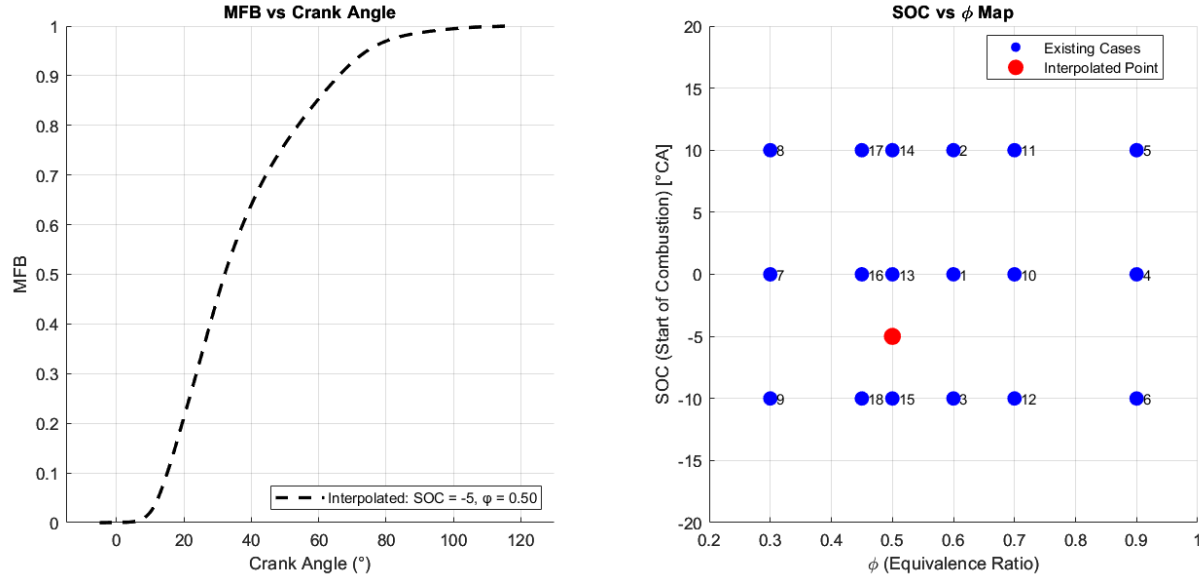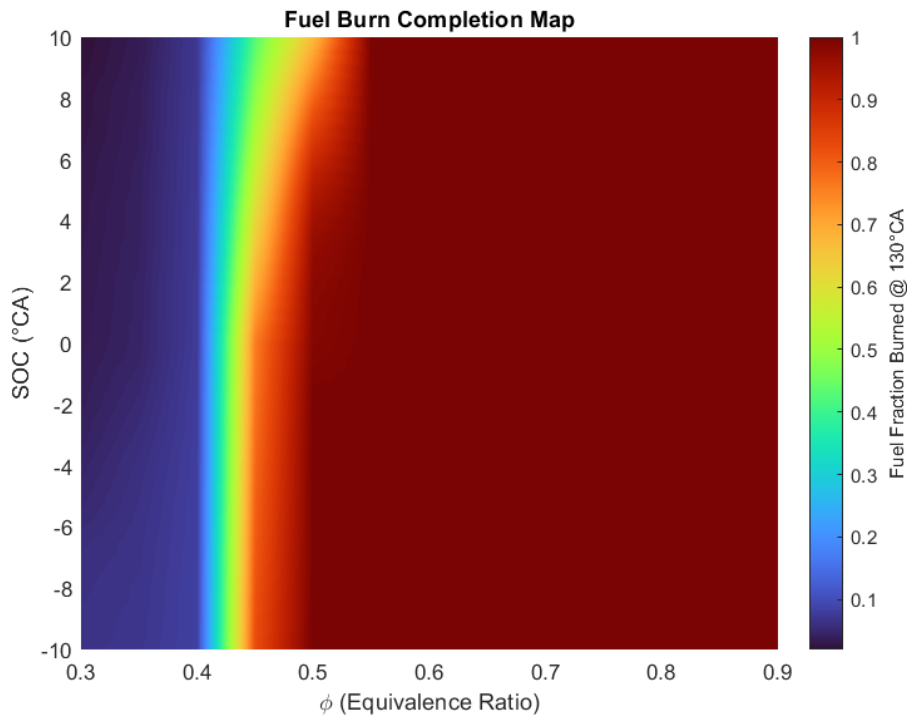
Figure 36: Example of interpolation on the spark timings (SOC=3° CA) for a fixed φ=0.5.

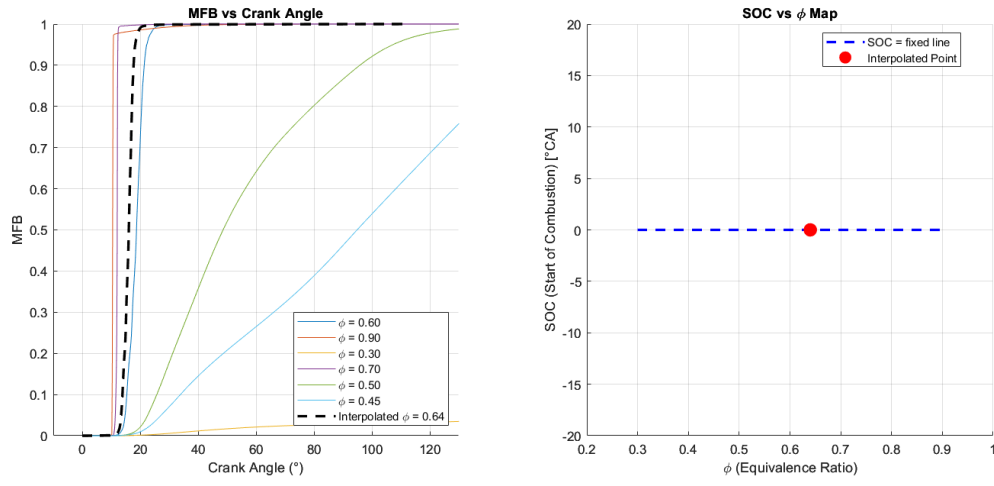By combining the two interpolation steps, a continuous 2D map of all possible MFB curves is generated. This 2D map enables the retrieval of an MFB curve for any combination of equivalence ratio $\phi \in [0.3, 0.9]$ and spark timing $SOC \in [-10°, 10°]$.
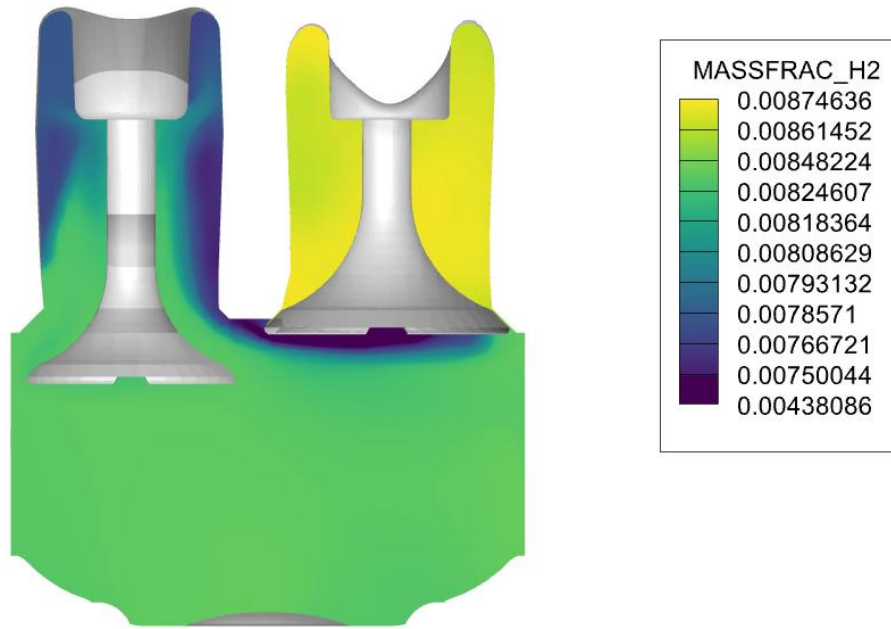
Figure 37: Example of an interpolated MFB curve (ϕ=0.5 ; SOC=-5° CA) across the whole 2D map.

The mass fraction burned can thus be represented continuously across this domain. This map is particularly valuable for identifying operating conditions where incomplete combustion occurs in the engine. Incomplete combustion is indicated when unburned fuel remains in the combustion chamber prior to EVO (130° CA). This phenomenon is detectable on the MFB map by curves that do not reach 100% completion, signaling incomplete combustion (see *Figure 38*).

Figure 38: 2D map of the fuel burn completion (Fuel Fraction burned at EVO = 130° CA).

Figure 39: Tecplot H2 fraction of an incomplete combustion (case 18) at EVO.

3.3.3 Importance of the CA50

CA50 refers to the crank angle at which 50% of the total fuel mass has been burned, i.e. the crank angle at which the MFB curve reaches 0.5. It is widely recognized as one of the most critical combustion parameters influencing engine efficiency. A preliminary investigation was carried out by fixing the φ=0.6 and varying the SOC to observe, within GT-Power, the effect of CA50 on engine performance. For this specific engine configuration, the results indicated that maximum efficiency is achieved when CA50 occurs at approximately 10° CA.
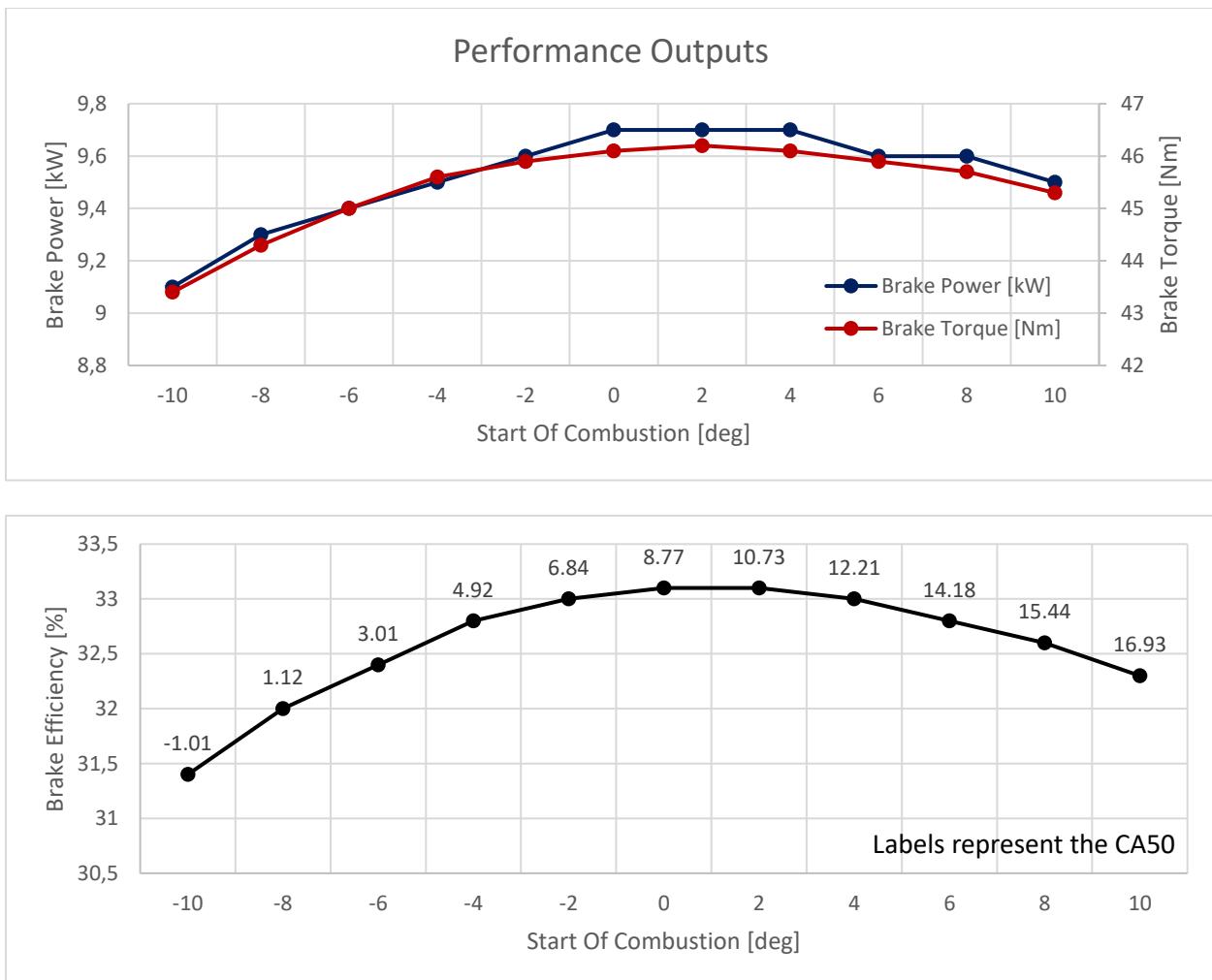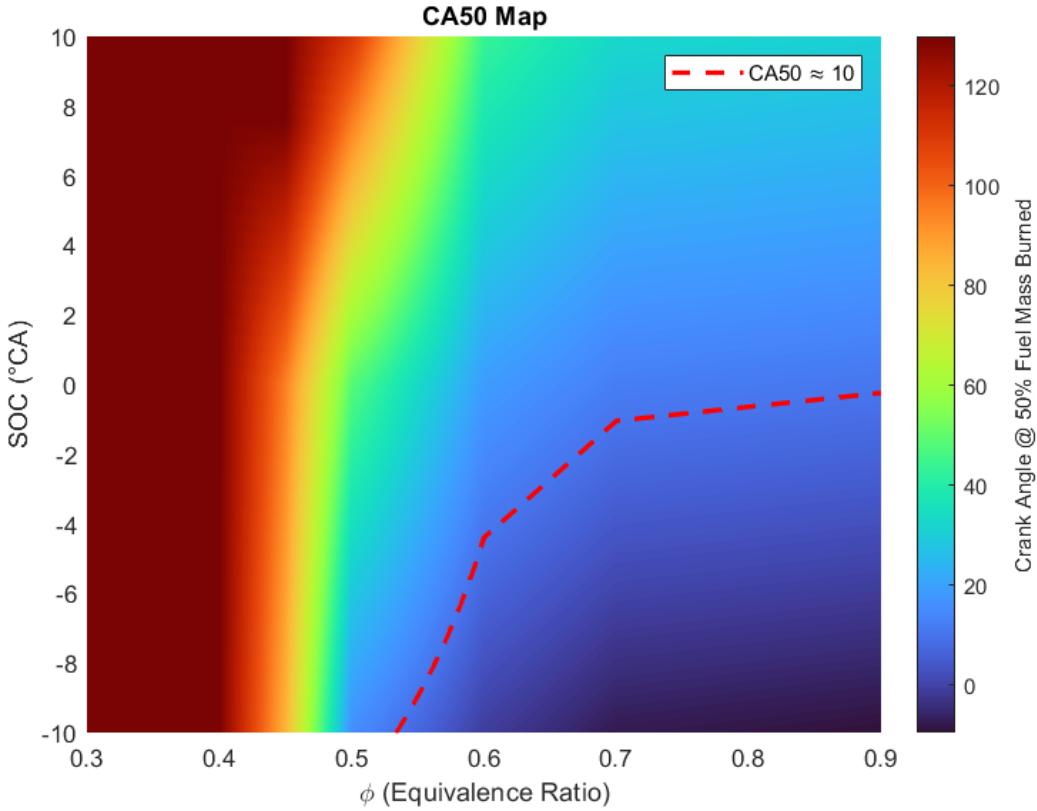
Figure 40: Performance Outputs for different SOC at φ=0.6 to find the most efficient CA50.

Since the engine achieves maximum efficiency at a constant CA50 of 10°CA, this value becomes the target for optimal operation across all conditions. Using the previously generated 2D MFB 2D map (see *Figure 37*), it is possible to determine the CA50 value for every combination of ϕ and SOC. By analyzing this map, the region corresponding to CA50=10° CA can be identified. This allows for the selection of operating points that maintain optimal combustion phasing, regardless of changes in ϕ or SOC (see *below*).
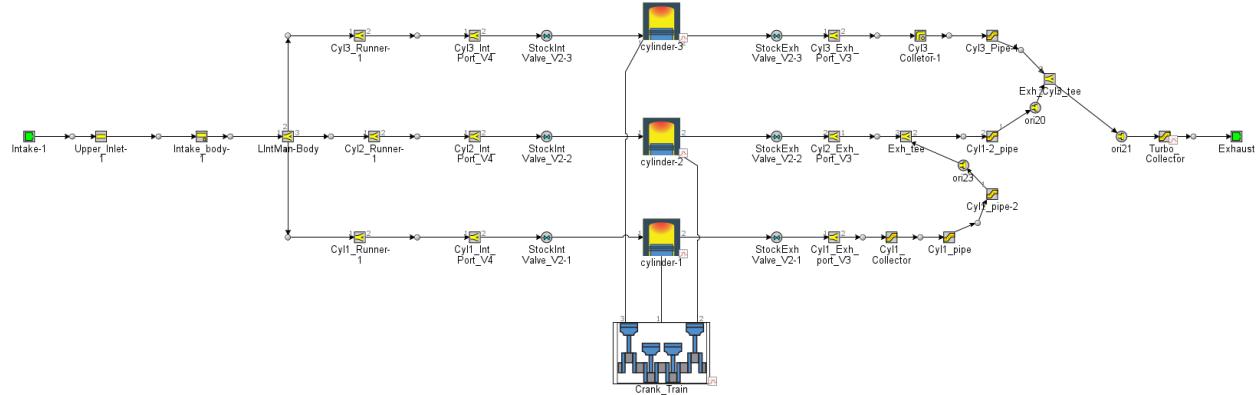
Figure 41: 2D map of the CA50 (Crank Angle when Mass Fraction burned MFB=50%).

3.4 1D Simulations

3.4.1   GT-Power Modelling Setup

The model is based on the work of Matthew Countie [3] for the geometry components. The intake and exhaust manifolds were already constructed in 3D and then converted into a 1D model using GEM3D, a tool developed by GAMMA Technologies LLC. The supercharger was removed from the original setup, as the current configuration focuses on a Naturally Aspirated (NA) engine. The engine geometry, including bore, stroke, and CR, was defined within the <u>EngineCrankTrain</u> object. Additionally, a detailed predictive friction model was implemented using the <u>EngFrictionGeom</u> object, which considers parameters such as bearing dimensions, oil viscosity, and piston ring friction. Although the model has not yet been calibrated, it relies on predictive elements, making it reasonably accurate for preliminary simulations. The details flow map is shown below in *Figure 42*.

Figure 42: GT-Power flow map of the predictive model.

3.4.2 Inputs to Build an Engine Model

The key advantage of building a fully predictive model is that it does not require real engine data for calibration, which simplifies the modeling process and reduces the number of necessary inputs. Additionally, the use of premixed fuel allows the modeling of fuel injectors to further streamlining the setup. The first set of required data is based on engine specifications, including:

- Crank-train geometry

- Block geometry

- Cylinder head geometry

- Piston geometry

- Intake and exhaust manifold geometry

- Valve lift profiles

Next, the engine operating conditions are defined, which include:

- Intake pressure and temperature

- Premixed fuel composition (via equivalence ratio)

- Combustion profile, defined by SOC MFB curve (more details in Section 3.4.3).

3.4.3 GT-Power Combustion Model

Rather than relying on the conventional EngCylCombSITurb or EngCylCombSIWiebe combustion models, this work employs a user-defined MFB profile through the EngCylCombProfile object. As demonstrated in Section 3.3.1, this approach enables the preservation of detailed combustion characteristics extracted from the 3D CFD simulations, ensuring a higher level of fidelity in the predictive 1D model. Furthermore, knock is modeled using the EngCylChemGas object, which allows the integration of a user-specified gas-phase chemical mechanism to enhance knock prediction accuracy.

3.4.4 Performance outputs

A total of 10 points were selected along the CA50 = 10 °CA iso-curve (see *Figure 41*), and for each of these operating points, the corresponding MFB curve was obtained through interpolation. These curves were then implemented in GT-Power using the EngCylCombProfile object. This approach ensures that the combustion profile used in the 1D simulation matches exactly the one predicted by the CFD analysis.

Table 11: Combinations of 10 (SOC ; Φ) with CA50 = 10° CA.

#	0	1	2	3	4	5	6	7	8
SOC	-10	-7.35	-4.52	-2.67	-1.1	-0.89	-0.67	-0.51	-0.28
Φ	0.53	0.57	0.6	0.65	0.7	0.75	0.8	0.85	0.9

After running the 10 simulation cases (see *Table 11*) with the imported MFB curves, the engine's performance was evaluated, most importantly, its power output, to determine whether it could theoretically achieve the target of 10 kW. Results indicate (see *Figure 43: Performance Outputs for different Φ of* the Table 11.) that the combination of ϕ=0.5 and SOC=−10° CA yields the maximum power with the highest efficiency for this specific engine configuration.

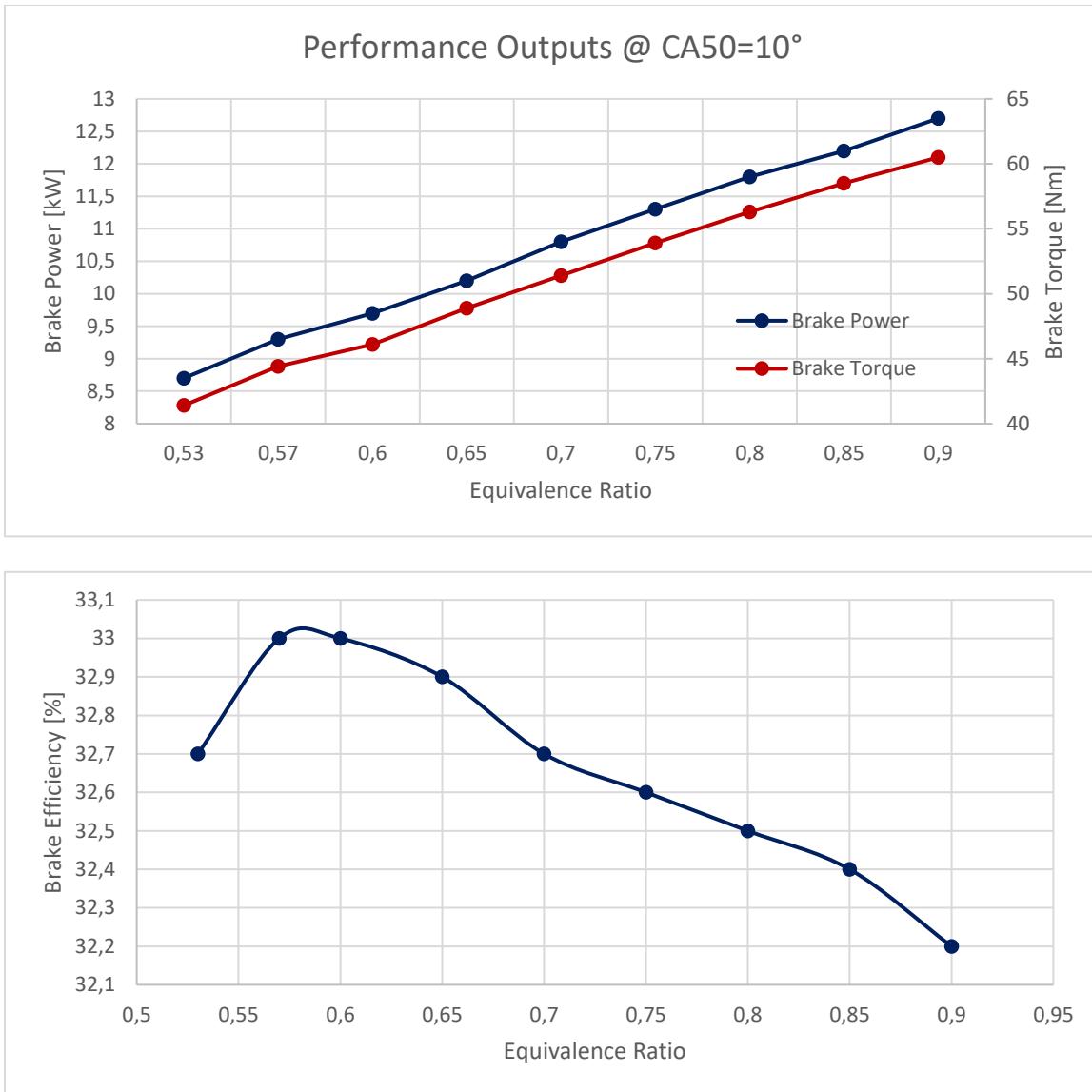*Figure 43: Performance Outputs for different Φ of the Table 11.*

The maximum peak pressure achieved in the cylinder for the redesigned piston head, operating at a CR of 10:1, is 5.5 MPa. As shown in the corresponding *Figure 20*, this peak pressure yields a SF of 3.19, thereby confirming the mechanical viability of the new piston geometry under the specified operating conditions.

4. SUMMARY AND CONCLUSION

The primary objective of this work was to convert a 1-liter diesel engine into a hydrogen-fueled PFI SI engine, while also developing a predictive method for estimating performance outcomes. The key achievements aligned with the initial goals presented in Section 1.3.1 can be summarized as follows:

- The pistons were redesigned to lower the compression ratio from 22.8:1 to 10:1, making them suitable for hydrogen combustion.

- FEA demonstrated that the redesigned pistons could withstand both thermal and mechanical stress under the new operating conditions, with a SF of 3.19.

- The combustion process was fully modeled on a 2D map through interpolation of 3D CFD simulation results.

- Simulations indicated that the engine could produce up to 10 kW of brake power with a thermal efficiency of approximately 30%, operating exclusively on pure hydrogen at standard temperature and atmospheric pressure.

- Finally, this work introduces an innovative methodology to predict engine performance without the need for physical testing. This approach is not only applicable to hydrogen-fueled engines but can also be extended to various engine types and fuel blends.

While the proposed method shows considerable promise, there remain areas for improvement. Notably, the current process is limited to fixed intake conditions (pressure and temperature).

As previously discussed, the entire process could be automated to enhance usability and streamline the workflow. This could be achieved by scripting the export of simulation results from CONVERGE CFD, feeding them directly into the MATLAB interpolation routine, and subsequently integrating the data into GT-Power.

Although the current model incorporates knock behavior through chemical kinetics, future studies could focus on a more detailed knock analysis, specifically to identify knock-limited regions on the 2D combustion map.

Finally, to validate the predictive capabilities of the proposed modeling framework, it is essential to compare the simulation results against experimental data from the actual converted engine. This comparison would also allow for an assessment of the accuracy and advantages of the proposed method relative to conventional GT-Power models, such as the TPA model.

5. REFERENCES

[1] Durkin, K.; Khanafer, A.; Liseau, P.; Stjernström-Eriksson, A.; Svahn, A.; Tobiasson, L.; Andrade, T.S.; Ehnberg, J. *Hydrogen-Powered Vehicles: Comparing the Powertrain Efficiency and Sustainability of Fuel Cell versus Internal Combustion Engine Cars*. Energies 2024, 17, 1085. https://doi.org/10.3390/en17051085.

[2] Robert J. Braun. *High Efficiency, Low Cost & Robust Hybrid SOFC/IC Engine Power Generator.* Colorado School of Mines, Golden, Colorado. Technical Volume DE-FOA-0001797.

[3] Countie, M. *Predictive Modeling and Testing of a Diesel Derived Solid Oxide Fuel Cell Tail Gas Spark-Ignition*. Department of Mechanical Engineering, Colorado State University. Summer 2020.

[4] Convergent Science webinar: *Converge for H2 Modelling: IC Engines*. 2025.

[5] Yong Li, Wenzhi Gao, Pan Zhang, Zhen Fu, Xingda Cao, *Influence of the equivalence ratio on the knock and performance of a hydrogen direct injection internal combustion engine under different compression ratios, International Journal of Hydrogen Energy*, Volume 46, Issue 21, 2021, Pages 11982-11993, ISSN 0360-3199, https://doi.org/10.1016/j.ijhydene.2021.01.031.

[6] European Aluminum Association. *The Aluminum Automotive MANUAL, Application-Powertrain-Pistons*. version 2011. auto@eaa.be.

[7] John B. Heywood. *Internal Combustion Engine Fundamentals*. McGraw-Hill Series in Mechanical Engineering. 1988.

[8] GAMMA Technologies LLC. *GT-ISE Help, Reference manual, flow, Engine (GT-Power) Components*. 2022

[9] Shijun Dong, Scott W. Wagnon, Luna Pratali Maffei, Goutham Kukkadapu, Andrea Nobili, Qian Mao, Matteo Pelucchi, Liming Cai, Kuiwen Zhang, Mandhapati Raju, Tanusree Chatterjee, William J. Pitz, Tiziano Faravelli, Heinz Pitsch, Peter Kelly Senecal, Henry J. Curran. *A new detailed kinetic model for surrogate fuels: C3MechV3.3*. Applications in Energy and Combustion Science 9 (2022) 100043, https://doi.org/10.1016/j.jaecs.2021.100043

APPENDIX A : KOHLER KDW1003 ENGINE SPECS

Diesel

Cooling	Liquid
Cylinders	Multiple
Shaft	Horizontal
Warranty	3-Yr Commercial

Engine Type Four-stroke inline, cast-iron block, aluminum cylinder head with overhead cam and integrated fuel injection system

Emissions EPA/CARB Tier 4-compliant

15.4-24 HP

KDW1003

MODEL		KDW702	KDW1003	KDW1404
GROSS POWER @ RPM	max. hp (kW)	15.4 (11.5) @ 3600	23.7 (17.7) @ 3600	24 (17.9) @ 2700
DISPLACEMENT	cu in (cc)	41.9 (686)	62.7 (1028)	83.7 (1372)
BORE	in (mm)		3 (75)	
STROKE	in (mm)		3.1 (77.6)	
CYLINDERS		2	3	4
PEAK TORQUE @ RPM	ft-lb (Nm)	25 (34) @ 2700	36.8 (50) @ 2600	51.6 (70) @ 1600
COMPRESSION RATIO			22.8:1	
DRY WEIGHT	lb (kg)	145.4 (66)	187.6 (85)	216 (98)
OIL CAPACITY	U.S. qt (L)	1.7 (1.6)	2.5 (2.4)	3.5 (3.3)
LUBRICATION		Full-pressure lubrication with full-flow filter		
DIMENSIONS L x W x H	in (mm)	16.6 x 16.2 x 20.3 (421 x 412 x 516)	20.2 x 16.2 x 20.3 (513 x 412 x 516)	23.5 x 16.2 x 20.3 (596 x 412 x 516)

APPENDIX B : AlSi12 MECHANICAL PROPERTIES

THE Aluminium Automotive MANUAL

	Eutectic Alloy AlSi12 CUMgNi		Hypereutectic Alloy AlSi18CuMgNi		Special Eutectic Alloy AlSi12Cu4Ni2Mg
	cast	forged	cast	forged	cast
Yield Strength $R_{p0.2}$ (MPa) at Temperature					
20°	190 – 230	280 – 310	170 – 200	220 – 280	200 – 280
150°	170 – 220	230 – 280	150 – 190	200 – 250	–
200°	120 – 170	–	100 – 150	–	150 – 200
250°	80 – 110	90 – 120	80 – 120	100 – 140	100 – 150
300°	50 – 80	–	60 – 80	–	85 – 100
Ultimate Tensile Strength R_m (MPa) at Temperature					
20°	200 – 250	300 – 370	180 – 230	230 – 300	210 – 290
150°	180 – 230	250 – 300	170 – 210	210 – 260	–
200°	160 – 200	–	160 – 190	–	170 – 210
250°	100 – 150	110 – 170	110 – 140	100 – 160	130 – 180
300°	80 – 100	–	90 – 130	–	100 – 120
Elongation to Fracture A_5(%)					
20°C	0,3 – 1,5	1 – 3	0,2 – 1,0	0,5 – 1,5	0,1 – 0,5
Hot Hardness after 200 hours at temperature: Hardness ($HB_{5/50/30}$)					
20°C	90 – 125	90 – 125	90 – 125	90 – 125	100 – 150
150°C	80 – 90	80 – 90	80 – 90	80 – 90	80 – 115
200°C	60 – 70	60 – 70	60 – 70	60 – 70	60 – 75
250°C	35 – 45	35 – 45	35 – 45	35 – 45	45 – 50
300°C	20 – 30	20 – 30	20 – 30	20 – 30	30 – 40
Fatigue Strength σ_w (N/mm^2)					
20°C	80 – 120	110 – 140	80 – 110	90 – 120	90 – 120
150°	70 – 110	90 – 120	60 – 90	70 – 100	90 – 120
250°	50 – 70	60 – 70	40 – 60	50 – 70	60 – 80
300°	–	–	–	–	45 – 60

Mechanical properties of piston alloys at various temperatures

Source: F. Rösch
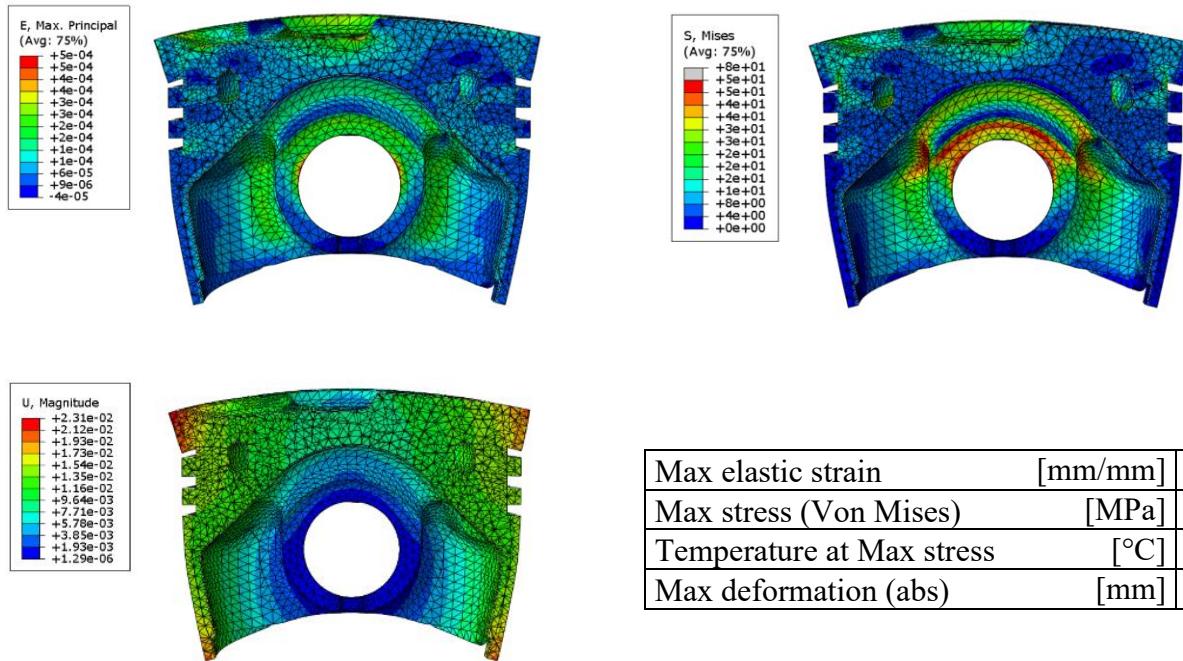
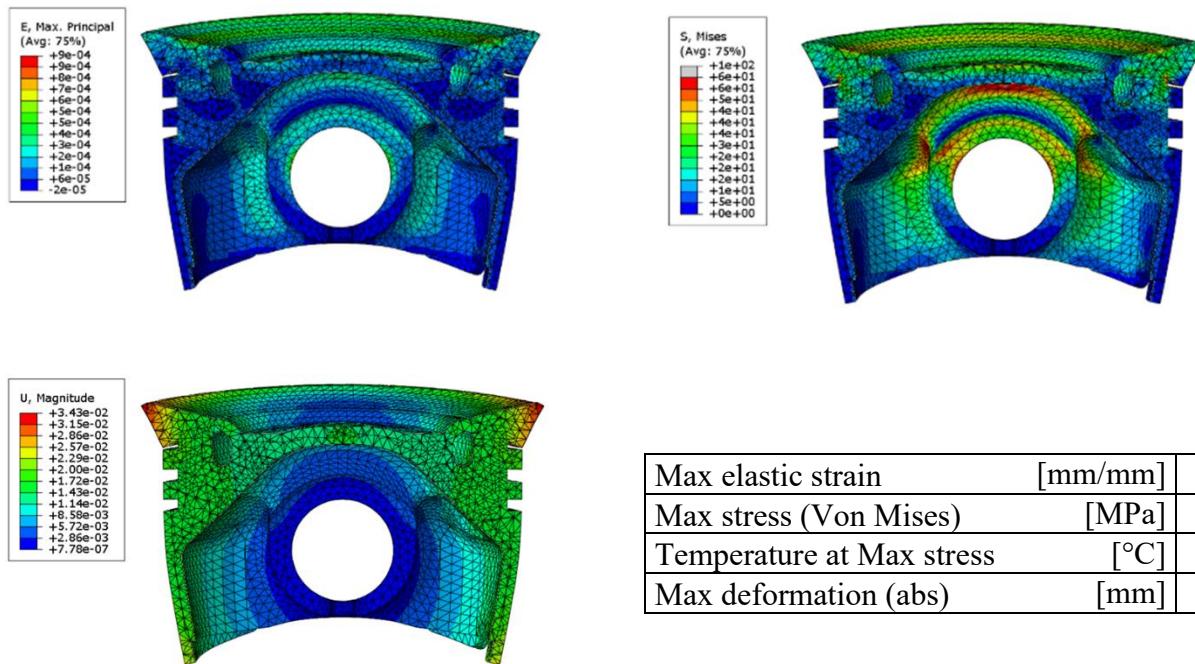|	Eutectic Alloy AlSi12 Cu MgNi		Hypereutectic Alloy AlSi18CuMgNi		Special Eutectic Alloy AlSi12Cu4Ni2Mg
	cast	forged	cast	forged	cast
Density (kg/dm^3)					
at 20°C	2.70	2.70	2.68	2.68	2.80
Linear thermal expansion coefficient (1/K)					
between 20° and 200°C	20.5 - 21.5	20.5 - 21.5	18.5 - 19.5	18.5 - 19.5	20.5 - 21.5
Thermal conductivity (W/cm · K)					
at 20°C	1.43 - 1.55	1.47 – 1.60	1.34 - 1.47	1.43 - 1.55	1.30 – 1.40
Specific heat (J/g · K)					
at 100°C	0.96	0.96	0.96	0.96	0.96
Youngs modulus (MPa)					
at 20°C	80.000 - 81.000	81.000	83.000 - 84.000	84.000	82.000
at 200°C	73.000 - 74.000	-	75.000 - 76.000	-	78.000
at 250°C	68.000 - 72.000	74.000	-	76.000	72.000
at 300°C	-	-	-	-	70.000

Physical properties of piston alloys

Source: F. Rösch

APPENDIX C : ABAQUS CAE PISTON FEA RESULTS

FEA Results original design (CR22.8:1)

Max elastic strain	[mm/mm]	5E-04
Max stress (Von Mises)	[MPa]	80
Temperature at Max stress	[°C]	150
Max deformation (abs)	[mm]	2.31E-02

FEA Results modified design (CR10:1)

Max elastic strain	[mm/mm]	9E-04
Max stress (Von Mises)	[MPa]	100
Temperature at Max stress	[°C]	200
Max deformation (abs)	[mm]	3.43E-02